Geologic Map of the Amboy Quadrangle, Clark and Cowlitz Counties, Washington

By Russell C. Evarts

Pamphlet to accompany
Scientific Investigations Map 2885

2005

U.S. Department of the Interior
U.S. Geological Survey

INTRODUCTION

GEOGRAPHIC AND GEOLOGIC SETTING

The Amboy 7.5' quadrangle is situated in the foothills of the western Cascade Range approximately 50 km northeast of Portland, Oregon (fig. 1). Since late Eocene time, the Cascade Range has been the locus of an active volcanic arc associated with underthrusting of oceanic lithosphere beneath the North American continent along the Cascadia Subduction Zone. Volcanic and shallow-level intrusive rocks emplaced early in the history of the arc underlie the Amboy quadrangle, forming a dissected and glaciated terrain with elevations as high as 2050 ft (625 m). The quadrangle is transected by two troughs that roughly parallel the east-west structural grain. The northern trough is occupied by Lake Merwin, an artificial reservoir inundating the valley of the Lewis River. The Lewis drains a large area in the southern Washington Cascade Range, including the southern flank of Mount St. Helens, approximately 20 km upstream from the quadrangle, before joining the Columbia River about 25 km west of the quadrangle (fig. 1). The southern trough, which includes Chelatchie Prairie and the lower stretch of Cedar Creek, probably marks a former course of the Lewis River.

The Amboy quadrangle lies east of the Portland Basin, which separates the Cascade Range from the Oregon Coast Range (fig. 1). The Portland Basin has been interpreted as a pull-apart basin located in the releasing stepover between two en echelon, northwest-striking, right-lateral fault zones (Beeson and others, 1985, 1989; Yelin and Patton, 1991; Blakely and others, 1995). These fault zones are thought to reflect regional transpression and dextral shear within the forearc in response to oblique subduction of the Pacific Plate (Pezzopane and Weldon, 1993; Wells and others, 1998). The southwestern margin of the Portland Basin is a well-defined topographic break along the base of the Tualatin Mountains, an asymmetric anticlinal ridge that is bounded on its northeast flank by the Portland Hills Fault Zone (Balsillie and Benson, 1971; Beeson and others, 1989; Blakely and others, 1995), which is probably an active structure (Wong and others, 2001; Liberty and others, 2003). The nature of the corresponding northeastern margin of the basin is less clear, but a poorly defined and partially buried dextral extensional structure has been inferred from topography, microseismicity, potential field-anomalies, and reconnaissance geologic mapping (Yelin and Patton, 1991; Beeson and others, 1989; Blakely and others, 1995).

This map is a contribution to a U.S. Geological Survey program designed to improve the geologic database for the Portland Basin region of the Pacific Northwest urban corridor, the densely populated forearc region of western Washington and Oregon. Better and more detailed information on the bedrock and surficial geology of the basin and its surrounding area is needed to refine assessments of seismic risk (Yelin and Patton, 1991; Bott and Wong, 1993), ground-failure hazards (Madin and Wang, 1999; Wegmann and Walsh, 2001) and resource availability in this rapidly growing region. The digital database for this publication is available on the World Wide Web at http://pubs.usgs.gov/sim/2005/2885.

PREVIOUS GEOLOGIC INVESTIGATIONS

Previous geologic mapping in the Amboy area, generally carried out as part of broad regional reconnaissance investigations, established the basic stratigraphic framework and distribution of geologic units in the quadrangle. The first systematic geologic work within the Amboy quadrangle was that of Mundorff (1964), who mapped the area south of the Lewis River to evaluate water resources in Clark County. He published a 1:48,000-scale geologic map and provided detailed descriptions of the basin-fill deposits. He later described the Pleistocene glacial deposits in the Lewis River valley, which he named the Amboy Drift (Mundorff, 1984).

Swanson and others (1993) updated Mundorff's (1964) Clark County work as part of an investigation of ground-water resources in the entire Portland Basin. Their work focused on the basin-fill units, and their map shows hydrogeologic rather than lithostratigraphic units, although there is substantial equivalence between the two. They analyzed lithologic logs of 1500 water wells to produce a set of maps that show the elevations and thicknesses of hydrogeologic units throughout the basin, thus constructing 3-dimensional view of the subsurface stratigraphy of the basin fill.

Phillips (1987) compiled a 1:100,000-scale geologic map of the Vancouver 30'x60' quadrangle, which includes the Amboy 7.5' quadrangle, as part of the state geologic map program of the Washington Division of Geology and Earth Resources (Walsh and others, 1987). Although relying heavily on Mundorff's work, he did undertake some original reconnaissance mapping. Phillips was the first to depict the Mount St. Helens-derived deposits in the lower Lewis River valley. He also mapped major stratigraphic units within the Tertiary bedrock sequence and acquired chemical analyses for some of the volcanic rocks of the region as well as a few whole-rock K-Ar age determinations. However, none of these new data were obtained from the Amboy quadrangle.

Topical geologic investigations in the Amboy quadrangle include those of Hyde (1975) and Major and Scott (1988), who described but did not map the Mount St. Helens-related deposits of the Lewis River valley, and Fiksdal (1975), who delineated several areas of potential slope instability in the quadrangle.

ACKNOWLEDGMENTS

Access granted by the many landowners was essential for mapping in the Amboy quadrangle. Robert Ross and Dennis Mohan of the Longview Fibre Company, Ross Graham and Dorothy Yount of Weyerhaeuser Company, and Ann Wikman and Brian Poehlein of the Washington Division of Natural Resources permitted work on their timberlands. Anna King, Richard Barney, and William Fields of PacifiCorp and Danny Walling of Lake Merwin Campers Hideaway permitted work on the lands adjacent to Lake Merwin. Diane M. Johnson of Washington State University performed chemical analyses and Robert Fleck of the U.S. Geological Survey provided $^{40}Ar/^{39}Ar$ ages. Bradley Reid, Zenon Valin, and Philip Dinterman gave able field assistance. Andrei Sarna-Wojcicki, Kenneth Bishop, Judith Fierstein, and Michael Clynne made available essential laboratory facilities. Water-well drillers' logs were examined in the offices of the Washington Department of Ecology Southwest Regional Office in Lacey, Wash., with the assistance of Stephanie Abraham and Tammy Howes. Connie Manson, librarian at the Washington Division of Geology and Earth Resources in Olympia, Wash., aided in obtaining information from that agency's files. I have benefited immensely from discussions on various aspects of the regional stratigraphy, structure, and geologic history of southwestern Washington with Roger Ashley, Michael Clynne, Paul Hammond, Keith Howard, Alan Niem, William Phillips, William Scott, James Smith, Donald Swanson, Karl Wegmann, and Ray Wells. Field and office consultations with Clynne were invaluable for interpreting Mount St. Helens-derived deposits. Detailed technical reviews by Clynne and Robert J. McLaughlin helped correct flaws and oversights in the original manuscript.

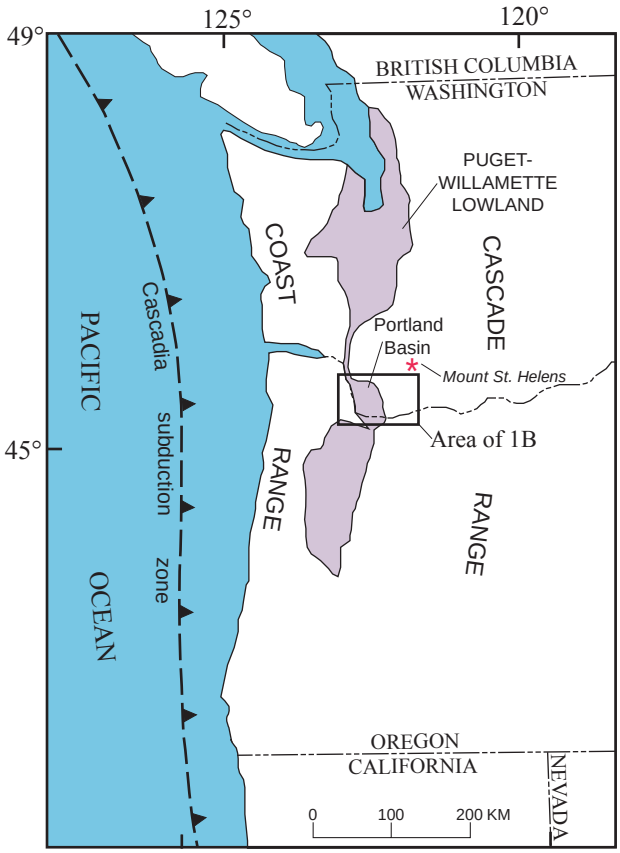

Figure 1A. Regional setting of the Amboy quadrangle showing major tectonic and physiographic features of the Pacific Northwest.

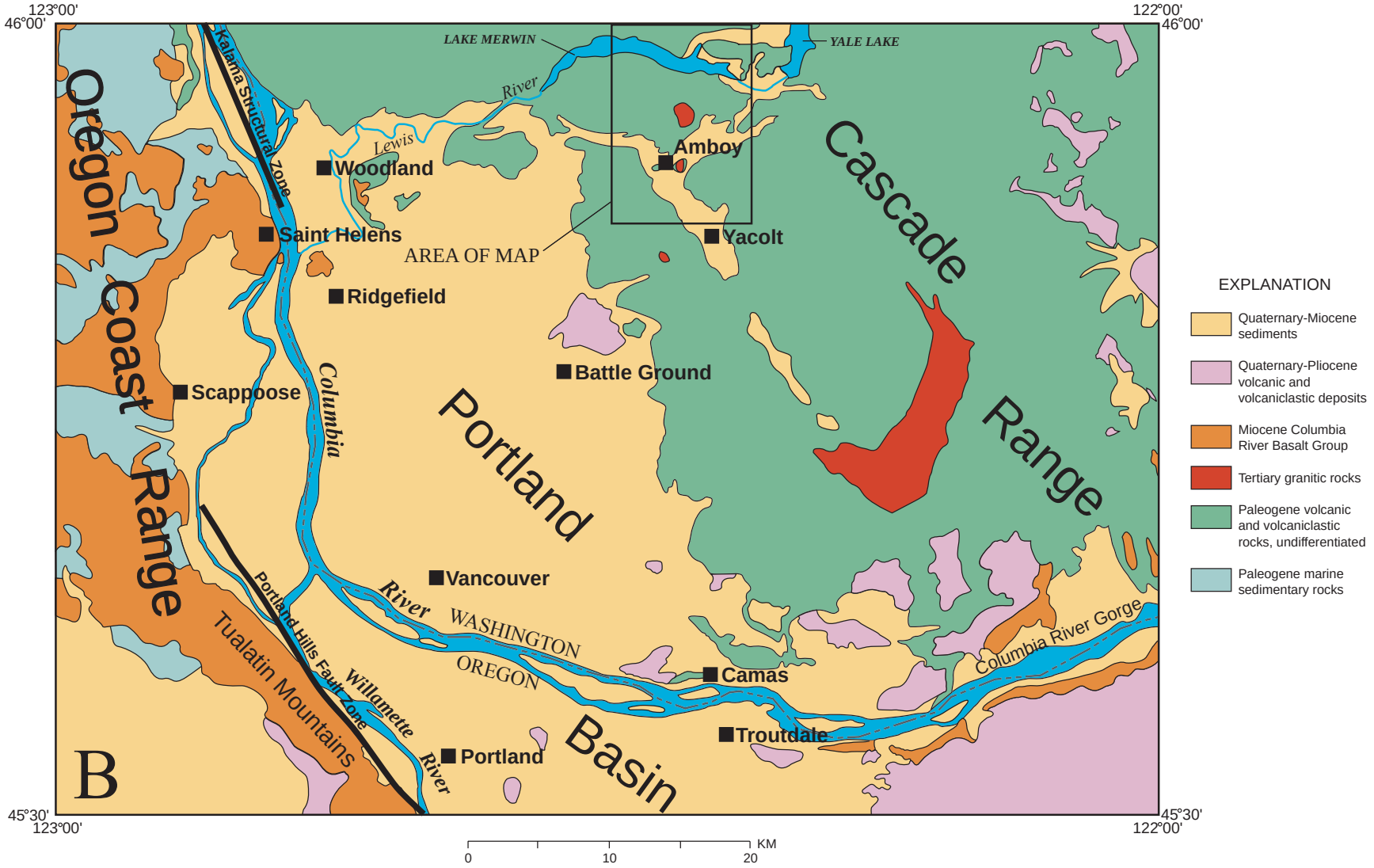

Figure 1B. Simplified geologic map of the Vancouver 30' x 60' quadrangle, modified from Phillips (1987a).

SYNOPSIS OF GEOLOGY

Bedrock of the Amboy quadrangle consists of a diverse assemblage of late Eocene and earliest Oligocene volcanic and volcaniclastic rocks that comprise early products of the Cascade volcanic arc. These strata strike east-west to northeast and dip to the south and southeast at low angles, generally less than 25°; dips generally decrease to the south. They are intruded by several plug-like or sill-like bodies of diorite and quartz diorite. The east-northeast trend of Chelatchie Prairie and the north-northwest-trending reach of Cedar Creek reflect control by fault zones.

During the Pleistocene, mountain glaciers repeatedly formed in the Lewis River valley (Crandell and Miller, 1974; Mundorff, 1984) and extended downvalley as far as the map area. The largest glacier(s) covered virtually the entire quadrangle, leaving behind a smoothly sculpted topography of bedrock hills and valleys mantled by variable thicknesses of drift. As the glacier receded, outwash accumulated in the valleys of the Lewis River and Cedar and Chelatchie Creeks. In post-glacial time, eruptions at the Mount St. Helens volcanic center periodically deposited large amounts of volcanic debris into the Lewis River that was transported downstream as lahars and flood deposits (Hyde, 1975; Major and Scott, 1988).

Because of the extensive drift cover and dense vegetation of the region, outcrops of bedrock in the map area are generally limited to steep cliff faces, landslide scarps, and streambeds; many exposures are in roadcuts and quarries. The surface information was supplemented with lithologic data obtained from several hundred water-well reports in the files of the Washington Department of Ecology; well locations were taken as described in the reports and were not field checked, and only wells considered reliably located were used to infer the distribution and thicknesses of units in the subsurface.

PALEOGENE BEDROCK

Bedrock in the Amboy quadrangle consists of a diverse assortment of subaerially erupted lava flows and volcaniclastic rocks that are typical of the strata that underlie much of the western slopes of the southern Washington Cascade Range (Evarts and others, 1987; Smith, 1993; Evarts and Swanson, 1994). Bedrock strata in the quadrangle generally strike east-west to northeast and dip south to southeast low angles, generally less than 25°. They are intruded by several fine- to coarse-grained intrusions of intermediate composition. A few fine-grained mafic dikes cut the section north of Lake Merwin but are sparse compared to adjacent areas to the west (Evarts, 2004a, b). $^{40}Ar/^{39}Ar$ age determinations (R.J. Fleck, written commun., 2000, 2001, 2002) obtained for extrusive rocks within this and adjacent quadrangles indicate that the bedrock section exposed in the map area is mostly of late Eocene age, between 38 and 33 m.y. old, but the uppermost strata in the southern third of the map area are as young as 27 m.y. old (early Oligocene). Ages of the intrusions are unknown but most are believed to be no younger than early Miocene based on their relatively shallow emplacement depths and on regional magmatic history (Evarts and Swanson, 1994).

Lithostratigraphic nomenclature for the stratigraphically complex Tertiary volcanic rocks of the southern Washington Cascade Range is poorly developed. Formal names have been proposed for Paleogene volcanic strata in several widely scattered locations (Wilkinson and others, 1946; Snavely and others, 1958; Roberts, 1958; Trimble, 1963; Fiske and others, 1963). However, these formations have proven to be only locally important or to be so broadly defined as to be merely synonymous with Tertiary volcanic rocks (Evarts and others, 1987; Smith, 1993). Phillips (1987) assigned the Eocene rocks north of Green Mountain to the Goble Volcanics of Wilkinson and others (1946), but Evarts (2002) showed that the criteria employed by Phillips to correlate these rocks with those of the type area are unreliable. In order to show as much detail as possible without generating a proliferation of local lithostratigraphic units, this map portrays primarily lithologic rather than lithostratigraphic units, although informal lithostratigraphic names are used where appropriate.

VOLCANIC AND VOLCANICLASTIC ROCKS

Basaltic andesite, andesite, and basalt

Mafic to intermediate lava flows and flow breccia are major components of the Paleogene section of the Amboy quadrangle. Most are about 5 to 10 m thick but some are as thick as 70 m. They are characterized by blocky to platy (rarely columnar) jointed interiors that grade into upper and lower flow breccia zones. Abundant zeolite- and clay-filled vesicles and reddish colors owing to oxidation during cooling typify upper flow breccia zones. All flows were apparently emplaced subaerially; many rest on red paleosols developed on interflow sediments and no pillow lavas or other indications of subaqueous environments were observed. The flows range in texture from

aphyric to densely porphyritic. Basaltic andesites (Tba and Tbem) typically contain phenocrysts of plagioclase, olivine, and augite in an intergranular to trachytic groundmass, whereas andesites contain phenocrysts of plagioclase, augite, and (or) hypersthene in an intersertal to pilotaxitic groundmass.

The basaltic andesite flows in the southern part of the map area (Tbem) are at the base of an extensive sequence of tholeiitic flows that extends about 65 km south to Camas (R.C. Evarts, unpub. mapping). This unit, informally named the basaltic andesite of Elkhorn Mountain, consists predominantly of plagioclase + olivine ± augite-phyric lavas; interbedded volcaniclastic rocks are generally sparse. $^{40}Ar/^{39}Ar$ ages of about 27 Ma were obtained from this unit in the Yacolt quadrangle to the south (R.J. Fleck, written commun., 2005). The basaltic andesite of Elkhorn Mountain is interpreted as a large mafic shield volcano, probably centered to the southeast of the map area. If this interpretation is correct, it implies that the base of the unit is an unconformity separating the 27-Ma basaltic andesite of Elkhorn Mountain from underlying strata that are about 33 m.y. old.

Basalt flows are uncommon in the Amboy quadrangle; two types are distinguished on this map. Isolated flows of aphyric and olivine+plagioclase-phyric basalt (Tb) crop out in the northern part of the quadrangle, low in the stratigraphic section. Flows of distinctive feldspar-free olivine-phyric basalt (Tob) are also largely restricted to the lower part of the Paleogene section. The olivine phenocrysts in these flows contain abundant euhedral inclusions of chromian spinel and, unlike those in other mafic rocks, are not completely altered. The lenticular unit, as thick as 150 m, that crops out on the steep north slope of Green Mountain consists largely of poorly sorted, indurated, brick-red scoria and likely represents a slice through the flank of a late Eocene cinder cone.

Dacite

Dacitic flows (Td) are dispersed throughout the upper part of the Paleogene stratigraphic section of the Amboy quadrangle. All are porphyritic pyroxene dacites similar to those found to the west (Evarts, 2004a, b).

Volcaniclastic rocks

Volcaniclastic rocks make up a substantial proportion of the Paleogene bedrock in the Amboy quadrangle. On this map they are divided into a unit of volcaniclastic sedimentary rocks of predominantly epiclastic origin (Tvs) and units comprised of mostly pyroclastic rocks (Tt and Tdpo). In addition, thin unmappable volcaniclastic beds commonly separate lava flows of units Ta, Tba, and Td. The volcaniclastic sedimentary rocks unit (Tvs) includes a diverse assemblage of generally well-bedded, texturally and compositionally immature siltstone, sandstone, conglomerate, and breccia. Fragments of volcanic rocks petrographically similar to interbedded lava flows are the dominant constituents of most beds; less abundant components include plagioclase, Fe-Ti oxides, and pyroxene crystals, pumice, vitric ash, fine-grained dioritic rocks, and plant remains. These beds include thin debris-flow and hyperconcentrated flood-flow (Smith, 1986) deposits as well as finer grained fluvial and lacustrine strata probably deposited beyond the flanks of volcanic edifices. In addition to material eroded from older extrusive rocks, these beds likely contain clasts reworked from unconsolidated penecontemporaneous airfall and ash-flow deposits.

The tuff unit (Tt) consists of andesitic to rhyolitic tuff, pumiceous and lithic lapilli tuff, and lithic tuff breccia that are inferred to be the direct products of explosive eruptions and volcanic debris flows. Most are medium to coarse grained, poorly sorted, matrix supported, and contain abundant originally vitric ash. Pumice-lapilli tuffs were presumably emplaced as pyroclastic flows, whereas more heterolithic, lithic-rich beds were probably deposited by lahars. Pumiceous tuffs north of Cedar Creek and Chelatchie Prairie tend to be weakly welded, sparsely phyric, and orange to brown, whereas those to the south are commonly densely welded and porphyritic. Phenocryst assemblages in most tuffs consist of plagioclase, augite, hypersthene, and Fe-Ti oxide; hornblende is very rare and no quartz or biotite were observed in any tuffs of this quadrangle. A densely welded and locally vitrophyric tuff (Tdpo) that crops out on the south side of Cedar Creek west of Amboy is believed to have been emplaced during a caldera-forming eruption in the Ariel quadrangle at about 35.1 Ma (Evarts, 2004b). Analysis of plagioclase from two welded tuffs at about the same stratigraphic position in the southern part of the map area yielded analytically indistinguishable $^{40}Ar/^{39}Ar$ ages of 33.4±0.4 Ma and 33.0±0.1 Ma (table 2).

INTRUSIVE ROCKS

In contrast to the adjacent Ariel quadrangle (Evarts, 2004b), fine-grained dikes are sparse in the Amboy quadrangle. They are found only in the lower part of the stratigraphic section near Lake Merwin. A 30-m-thick sill of strikingly plagioclase-phyric basalt forms a prominent cliff on the steep valley wall south of Speelyai Creek. This sill is petrographically and chemically similar to some flows in the Paleogene section north of the Amboy quadrangle (Evarts and Ashley, 1991). Several hypabyssal intrusions of mafic to intermediate composition are

present south of Lake Merwin. The largest are sill-like bodies at Dunegan Mountain (Tdid) and north of Buncombe Hollow Creek (Tdib) and a cylindrical body of fine- to medium-grained porphyritic diorite at the southwest end of Chelatchie Prairie (Tdic). The Dunegan Mountain intrusion is composed of relatively uniform medium-grained augite diorite in which feldspar is extensively replaced by stilbite. The long sill that crops out between Lake Merwin and Buncombe Hollow Creek is a composite body comprising several intrusions of porphyritic to seriate pyroxene diorite. Most of the smaller intrusions in the map area are sill-like bodies of relatively fine-grained diorite.

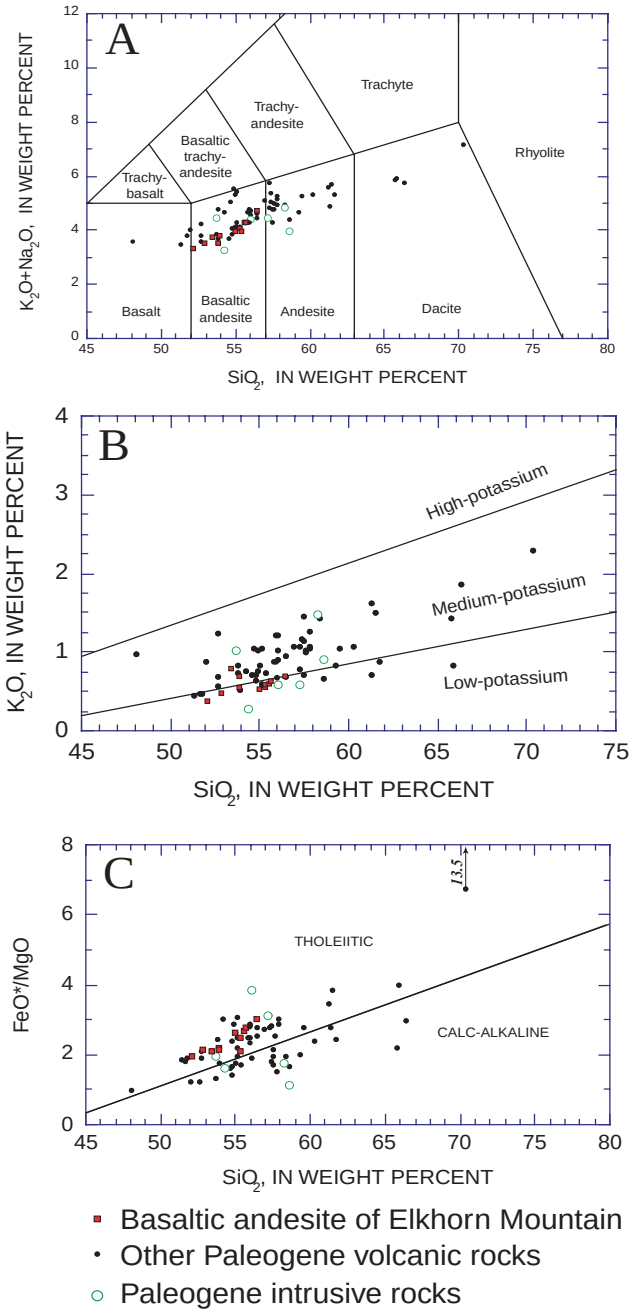

Figure 2. Chemical characteristics of volcanic rocks from the Amboy 7.5' quadrangle (analyses recalculated volatile-free). A, K_2O+Na_2O versus SiO_2 showing IUGS classification (Le Maitre, 2002); B, K_2O versus SiO_2 showing low-, medium-, and high postassium fields extrapolated from Gill (1981, p. 6); C, FeO*/MgO versus SiO_2, showing classification into tholeiitic and calc-alkaline rocks according to Miyashiro (1974). FeO*, total Fe as FeO.

None of the intrusions has been radiometrically dated. The fine-grained dikes (Tib, Tiba, Tia) compositionally and texturally resemble their late Eocene host rocks and are probably not much younger. The coarse grain size of some of the larger intrusions is consistent with slow cooling at depth, which implies that they are considerably younger than the volcanic host rocks.

ROCK CHEMISTRY

The chemistry of Paleogene lava flows and intrusive rocks in the Amboy quadrangle (table 1) is generally similar to that of Tertiary igneous rocks sampled elsewhere in the southern Washington Cascade Range (Evarts and Ashley, 1990a,b, 1991, 1992; Evarts and Bishop, 1994; Evarts and Swanson, 1994; Evarts, 2001, 2002, 2004a, b; R.C. Evarts, unpub. data). Compositions of igneous rocks in the quadrangle range from basalt to high-silica dacite and form a low- to medium-potassium suite (fig. 2). Analyses straddle the dividing line between tholeiitic and calc-alkaline compositions using the classification of Miyashiro (1974; fig. 2C). TiO_2 contents of some basaltic andesites and andesites are as high as 2.25 wt percent, commonly greater than in rocks to the west (Evarts, 2004a, b) and somewhat higher than is typical for volcanic-arc magmas (Gill, 1981). Some basalts and a thick sill in the lower part of the section north of Lake Merwin contain relatively low contents of large-ion lithophile elements (K, Ba, Sr) and thus resemble low-potassium tholeiites of the basalt of Kalama River that crop out to the north in the Lakeview Peak quadrangle (Evarts and Ashley, 1991). Flows in the basaltic andesite of Elkhorn Mountain are tholeiitic (fig. 2C) and are generally higher in Fe and lower in K_2O (fig. 2B) than basaltic andesites elsewhere in the map area; most are relatively poor in Sr (table 1 and R.C. Evarts, unpub. data). Many flows in the Elkhorn Mountain unit are abundantly plagioclase-phyric, as reflected in Al_2O_3 contents greater than 19 wt percent (table 1), and probably accumulated excess feldspar in a subvolcanic magma chamber prior to eruption. No consistent

chemical differences between eruptive and hypabyssal intrusive rocks are apparent (fig. 2).

METAMORPHISM AND HYDROTHERMAL ALTERATION

Paleogene rocks in the Amboy quadrangle have been subjected to zeolite-facies regional metamorphism, the general character of which is similar to that described from other areas in the southern Washington Cascade Range (Fiske and others, 1963; Wise, 1970; Evarts and others, 1987; Evarts and Swanson, 1994). This region-wide metamorphism reflects burial of the late Eocene and early Oligocene rocks by younger volcanic rocks within the relatively high-heat-flow environment of an active volcanic arc.

The extent of replacement of igneous minerals by secondary phases ranges from incipient to complete. Permeable, glass-rich, silicic volcaniclastic rocks are the most susceptible to zeolitization, whereas massive lava flows may be only slightly affected. In mafic to intermediate-composition lava flows, the primary effect of very-low-grade metamorphism is the nearly universal development of clay minerals and zeolites that replace labile interstitial glass, fill vesicles, and coat joint surfaces. Feldspar typically displays partial alteration to clay minerals and (or) zeolites. Olivine phenocrysts in most basalts and basaltic andesites are totally replaced by smectite with or without hematite and calcite; however, replacement is incomplete in some olivine-rich flows. Primary augite and Fe-Ti oxides are largely unaffected by the zeolite-facies metamorphism. Hypersthene phenocrysts in pyroxene andesite flows commonly exhibit minor replacement by dark brown smectite. In pervasively altered volcaniclastic rocks and flow breccias, smectitic clay minerals and zeolites pseudomorphically replace most framework grains and fill pore spaces; the development of iron-rich smectites gives these rocks their characteristic green colors. The widespread presence of heulandite and clinoptilolite in the volcaniclastic rocks of the map area indicates that, except for areas near intrusions, metamorphic temperatures did not exceed 180°C (Cho and others, 1987).

QUATERNARY DEPOSITS

The character of Quaternary sedimentation in the Amboy quadrangle has been shaped primarily by two processes: mountain glaciation and eruptions of the Mount St. Helens volcanic center. Alternating episodes of aggradation and incision have produced a complex series of terraces along the Lewis River.

GLACIAL AND RELATED DEPOSITS

Several times during the Pleistocene epoch, icecaps covered the Washington Cascade Range and spawned glaciers that moved down all of the major river valleys. From examinations of glacial deposits near Mount Rainier, Crandell and Miller (1974) inferred four major glacial episodes, each of which apparently consisted of several lesser advances and retreats (Dethier, 1988). The most widespread glacial deposits in the range are those related to the penultimate glaciation, the Hayden Creek Drift of Crandell and Miller (1974). Deeply weathered older deposits are locally preserved in the western Cascade foothills in areas beyond the reach of Hayden Creek glaciers. The last major glaciation in western Washington was the late Wisconsinan Fraser glaciation. Deposits of this age in the Cascade Range, named the Evans Creek Drift, are much less extensive than those of the Hayden Creek age (Crandell and Miller, 1974; Crandell, 1987). Widely distributed till and glaciofluvial sediments in the lower Lewis River valley were named the Amboy Drift by Mundorff (1984), who correlated them with the Hayden Creek Drift of the Mount Rainier region on the basis of similar weathering characteristics. Crandell (1987) noted that some of the till in Mundorff's (1984) Amboy Drift, however, was more deeply weathered than typical Hayden Creek Drift and suggested that the Amboy Drift as mapped by Mundorff (1964, 1984) includes some older drift (Crandell, 1987; see also Howard, 2002 and Evarts, 2004b). Most of the drift in the Amboy quadrangle appears to belong to the less weathered drift. It is therefore mapped as Amboy Drift and considered correlative with the Hayden Creek Drift of Crandell and Miller (1974). Some deposits are more deeply weathered, however, and are probably equivalent to the older drift noted by Crandell (1987).

Intensely weathered bouldery till and gravel (Qmt) are exposed near the southwest corner of the map area. They are correlated with similar deposits in the Ariel quadrangle that Evarts (2004b) mapped and informally named the drift of Mason Creek. These deposits are characterized by soil horizons more than 3 m thick and development of weathering rinds as thick as 1 cm or more on volcanic clasts. The area underlain by this drift is surrounded by the younger Amboy Drift. The younger Amboy-age glacier, which terminated about 3 km west of the quadrangle boundary, must have overridden this area, but it was apparently partially deflected by the bedrock ridge north of Maple Pit and thus unable to remove this patch of older drift. The age of the drift of Mason Creek is unknown.

Crandell (1987) suggested that the till along Mason Creek may be slightly older than the type Wingate Hill Drift of Crandell and Miller (1974), estimated to be from 300 to 600 ka (Colman and Pierce, 1981; Dethier, 1988). To the west, the drift of Mason Creek contains clasts probably eroded from basaltic flows emplaced between 600 ka and 800 ka (Evarts, 2004b).

As described by Mundorff (1964, 1984), the Amboy Drift includes till, stratified drift, outwash, and ice-contact deposits. Excellent exposures are found at many places along the shores of Lake Merwin. An extensive blanket of Amboy Drift till (Qat) covers much of the quadrangle to elevations as high as 1860 ft (565 m). At its maximum extent, Amboy-age ice buried all of the map area except the summit of Green Mountain. The terrain south of Green Mountain exhibits a distinctive topography composed of streamlined bedrock-cored hills (rock drumlins) with thin till mantles. The hills consist of south-dipping lava flows and were sculpted as the ice moved westward, parallel to strike, and preferentially excavated less resistant volcaniclastic interbeds. Some till outcrops in the Lewis River valley contain minor but conspicuous clasts of light-colored, coarsely porphyritic dacite bearing phenocrysts of quartz, cummingtonite, and biotite; such clasts are particularly common in till north of the Lewis River. These rocks have chemical and mineralogical affinities with products of the ancestral volcanic center at Mount St. Helens, which is the only known source in the Lewis River drainage for the distinctive dacite.

Deposits of stratified sand and gravel underlie Chelatchie Prairie and form terrace assemblages in the Lewis River and Cedar Creek valleys. These deposits (Qao) locally overlie till. Clast compositions and weathering characteristics are similar to those of the till, and the sediments are interpreted as glaciofluvial outwash deposited during retreat of Lewis River glacier in late Pleistocene time. The outwash appears to represent at least three aggradational episodes during recession of the Amboy-age glacier. The oldest outwash is that with a surface elevation of about 720 ft (220 m) near the south boundary of the map area. These glaciofluvial deposits are at the north end of a broad, flat-bottomed, gently south-sloping valley, occupied by the town of Yacolt, that was apparently filled with outwash when glacial ice still occupied Chelatchie Prairie and terrain to the north. Chelatchie Prairie declines from about 600 ft (180 m) at its east end to about 400 ft (120 m) near Amboy and is the surface of a valley train, locally as thick as 66 m, that was deposited when the glacier had receded to near the site of Yale Dam east of the Amboy quadrangle. The outwash deposits near the east end of Lake Merwin are probably of the same age. At its western end the surface of Chelatchie Prairie is inset against an older fill with a surface about 12 to 15 m higher. This older fill continues westward as semicontinuous terraces along Cedar Creek all the way to its mouth (Evarts, 2004b); these deposits may be approximately the same age as those beneath Yacolt.

The lake deposits (Ql) near the southwest corner of the quadrangle mark the east end of a proglacial lake impounded by Amboy-age terminal moraines (Grigg and Whitlock, 2002; Evarts, 2004b).

The numerical ages of Hayden Creek Drift and its local equivalent, the Amboy Drift, are poorly known. Estimates range from 60 ka to greater than 300 ka (Crandell and Miller, 1974; Colman and Pierce, 1981; Dethier, 1988). A minimum age comes from evidence in the Fargher Lake area of the adjacent Ariel quadrangle (Grigg and Whitlock, 2002) that suggests ice last covered the map area during marine oxygen-isotope stage (MIS) 4 (74 to 60 ka; Martinson and others, 1987). This is consistent with the lack of Cougar-age (21,000 to 18,000 yrs B.P.; fig. 3) Mount St. Helens rocks in the drift and with the presence of Evans Creek-age moraines about 70 km upriver (Crandell, 1987).

As noted by Mundorff (1984), in many places the Amboy Drift is overlain by as much as 2 m of weathered yellowish-gray tephra. The tephra contains quartz, biotite and cummingtonite, and is mineralogically similar to tephra set C of Mullineaux (1996). Tephra set C was erupted from Mount St. Helens during the volcano's Ape Canyon eruptive stage, which extended from about 36,000 to 50,000 ^{14}C years B.P. (fig. 3); there is no other source known in the Cascade Range for tephra with this mineralogy. Crandell (1987) believed that all activity at the volcanic center postdated the Hayden Creek glaciation, which he correlated with MIS 4. However, clasts of quartz+biotite±cummingtonite-bearing dacite are widespread in the Amboy Drift, documenting preglacial or synglacial eruptive activity at the ancestral volcanic center. Furthermore, data for ash beds in eastern Washington (Berger and Busacca, 1995; Whitlock and others, 2000) as well as recent geochronologic work at Mount St. Helens (Evarts and others, 2003) indicate that eruptive activity at Mount St. Helens probably began well before 100 ka. Thus some of the quartz+biotite±cummingtonite-bearing tephra may be much older than 50 ka, and the underlying till could correlate with MIS 6, about 130 to 190 ka (Martinson and others, 1987), or an even older glacial period. At a locality on the crest of Green Mountain, quartz+biotite±cummingtonite-bearing tephra rests on weathered bedrock and is overlain by till. Plagioclase in this tephra yielded an ^{40}Ar/^{39}Ar age of 250±36 ka (table 2), providing a maximum age for the peak of the Amboy/Hayden Creek glaciation. This is similar to the ^{40}Ar/^{39}Ar age of 270±20 ka for syneruptive ice-contact deposits in the Ariel quadrangle, which were also deposited when the Amboy-age Lewis River glacier was near its maximum extent (Evarts and others, 2003; Evarts, 2004b). These ages suggest that the Hayden Creek glaciation in the southern Washington Cascade Range corresponds to MIS 8, about 245 to 300? ka

(Martinson and others, 1987). It is possible, perhaps likely, that the deposits mapped here as Amboy Drift are diachronous and were actually deposited during more than one of the three glacial pulses of the Hayden Creek glaciation inferred by Dethier (1988) from an analysis of outwash-terrace deposits in the Cowlitz River valley, about 65 km north of the Amboy quadrangle.

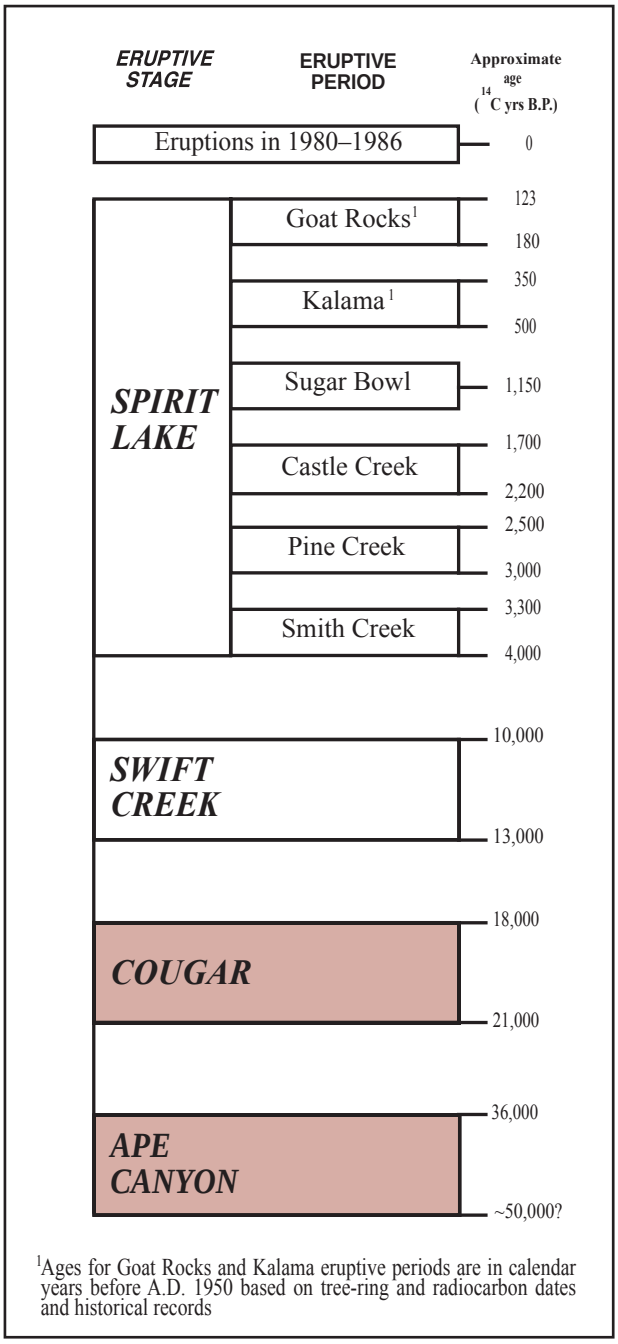

Figure 3. Eruptive stages and eruptive periods of Mount St. Helens volcano, modified from Crandell (1987). Shaded boxes designate stages corresponding to mapped deposits in the Amboy 7.5' quadrangle.

DEPOSITS DERIVED FROM THE MOUNT ST. HELENS VOLCANIC CENTER

The Lewis River drains the southern and eastern slopes of Mount St. Helens. Explosive eruptions at the volcanic center delivered large quantities of dacitic debris in the form of pyroclastic flows and lahars to the river during the late Pleistocene and Holocene (Crandell, 1987; Major and Scott, 1988). In postglacial time, eruptive activity at the volcano has been the dominant influence on sedimentation in the Lewis River valley. The periodic influx of volcaniclastic debris triggered major aggradational episodes downstream, and the deposits of these approximately syneruptive sedimentation events constitute a major part of the late Quaternary record in the lower Lewis River valley. Crandell (1987) showed that eruptive activity at Mount St. Helens was episodic and can be divided into several eruptive stages and periods (fig. 3). Based chiefly on their stratigraphic position and lithologic characteristics, Mount St. Helens-derived deposits in the Amboy quadrangle are assigned to Crandell's Ape Canyon and Cougar eruptive stages (fig. 3).

During the Ape Canyon eruptive stage, the Mount St. Helens volcanic center produced a distinctive white, coarsely porphyritic dacite containing phenocrysts of quartz and biotite (Crandell, 1987; Mullineaux, 1996). Major and Scott (1988) describe stratified, pumice-rich, alluvial sand and pebble gravel composed of this rock type (Qsa) from a narrow terrace along the north shore of Lake Merwin near Woodland Park. To the east, at the mouth of Rock Creek, a diamict that overlies west-dipping glaciofluvial beds contains boulders of quartz- and biotite-phyric dacite and may be a lahar deposit of about the same age as the alluvium. Poorly exposed Ape Canyon-age deposits also appear to underlie the dissected terrace surface at about 400 ft (120 m) elevation directly east of Lake Merwin. Sparse roadcut exposures show that these deposits include several meters of quartz- and biotite-bearing tephra as well as lithologically similar sandy alluvium. The scattered outcrops of Ape Canyon-age deposits indicate that during Ape Canyon time the lower Lewis River valley contained an extensive fill of volcaniclastic debris from the Mount St. Helens volcanic center.

Thick beds of sandy to gravelly alluvium and interbedded debris-flow deposits (Qsc) underlie a terrace surface inset into and about 15 m lower than that underlain by Ape Canyon-age deposits at the east end of Lake Merwin. Similar deposits underlie the valley of Speelyai Creek and form small terraces scattered along both shores of Lake Merwin farther west (Major and Scott, 1988; Evarts, 2004b). In several places these deposits unconformably overlie Amboy Drift. The debris-flow beds are poorly sorted and heterolithologic, composed predominantly of light-colored porphyritic dacites like those erupted from ancestral Mount St. Helens as well as variable proportions of Tertiary volcanics. These deposits probably formed from lahars that incorporated alluvium during transport. Major and Scott (1988) inferred these deposits to be largely of Cougar age (21,000 to 18,000 ^{14}C years B.P.), locally overlain by a few meters of Swift Creek-age (13,000 to 10,000 ^{14}C years B.P.) beds. This inference was based on the degree of soil development, the presence of abundant clasts of dacite similar to that erupted during Crandell's Cougar eruptive stage, and an age of 22,720±1,400 ^{14}C years B.P. that was obtained for charcoal in alluvium from the upper part of the Speelyai fill. Recent work by M.A. Clynne (written commun., 2003, 2004) indicates that clast compositions in the debris-flow beds are generally consistent with a Cougar age although some of these deposits could be older.

Few deposits younger than the Cougar eruptive stage have been identified in the Lewis River valley downstream from Mount St. Helens. A Swift Creek-age lahar is exposed below Merwin Dam in the Ariel quadrangle (Evarts, 2004b) and alluvium with young (<1,000 years B.P.) radiocarbon ages is present near the mouth of the river at Woodland (Major and Scott, 1988). Extensive deposits of the Swift Creek and Spirit Lake eruptive stages (fig. 3) may underlie the submerged Lewis River floodplain beneath Lake Merwin.

LANDSLIDE, TALUS, AND ALLUVIAL DEPOSITS

Landslide (Qls) and talus deposits (Qt) are common beneath cliffs in the Amboy quadrangle. Notable accumulations of talus have formed below the glacially steepened north flanks of the east-west-trending cuestas of Green Mountain and the ridge south of Speelyai Creek and on the east side of Dunegan Mountain. Most landslides result from failure of weathered, clayey, Paleogene volcaniclastic rocks (Tvs, Tt, and sedimentary interbeds within flow-dominated units Tba, Tbem, and Ta). Younger poorly lithified deposits are also susceptible to sliding, especially on steeper slopes. Only the larger landslides are shown on this map; many areas underlain by unconsolidated Quaternary units contain small slumps and debris-flow deposits that are too small to portray at 1:24,000 scale.

Unconsolidated alluvium (Qa) forms local and ephemeral accumulations along the active courses of Speelyai and Cedar Creeks and small alluvial cones at the base of steep gullies on the north slope of Green Mountain. Some areas mapped as alluvium, such as along Buncombe Hollow Creek and near the southeast corner of

the quadrangle, are the former channels of glacier-margin streams and these deposits are probably largely of Pleistocene age.

STRUCTURAL FEATURES

The Amboy quadrangle lies a few kilometers east of the northeastern margin of the Portland Basin, part of Puget-Willamette Lowland that separates the Cascade Range to the east from the Oregon and Washington Coast Ranges to the west. In the Cascade Range of southwestern Washington, structural attitudes of Paleogene strata delineate a set of large-wavelength, south- to southeast-plunging folds that are believed to have developed in late early Miocene time (Evarts and Swanson, 1994). The late Eocene and Oligocene section in the northern part of the Amboy quadrangle, which generally strikes approximately east-west and dips south at 15 to 30°, is located on the west limb of one of these folds, the Lakeview Peak anticline of Phillips (1987). A poorly defined synclinal axis lies in the Ariel quadrangle to the west (Evarts, 2004b). The Tertiary section flattens south of Cedar Creek, where dips are generally less than 15°, and is significantly disrupted by faulting near Chelatchie Prairie. In the southern part of the map area and to the south (R.C. Evarts, unpub. mapping) the basaltic andesite of Elkhorn Mountain is nearly flat-lying. This suggests that a slight angular discordance (<10°) exists between this unit and underlying strata, possibly indicating minor folding during the approximately 6 m.y. hiatus represented by the unconformity at its base.

Owing to limited outcrop, compelling evidence for the existence of faults in the Amboy quadrangle is sparse. Some faults shown on this map are projected from structures observed in roadcuts or natural exposures. Others have been inferred from apparent discontinuities in distinctive stratigraphic units, from topographic lineaments, or from abrupt changes in bedding trends. Most appear to be minor high-angle normal and strike-slip or oblique-slip faults of the kind characteristic of southwestern Washington (Wells, 1981; Wells and Coe, 1985; Evarts and Ashley, 1991, 1992; Evarts and Swanson, 1994; Evarts, 2002, 2004a, b; R.C. Evarts, unpub. mapping). Collectively, these structures presumably accommodated the paleomagnetically recorded rotations of small crustal blocks in response to long-term oblique convergence along the Cascadia Subduction Zone throughout Cenozoic time (Wells and Coe, 1985; Wells, 1989, 1990; Beck and Burr, 1979; Bates and others, 1981; Hagstrum and others, 1999).

As suggested by Mundorff (1964), major fault zones appear to be responsible for the northeast-striking basin of Chelatchie Prairie and the north-northwest-trending reach of Cedar Creek. The north-northwest-striking faults in the Cedar Creek area are inferred to be right-lateral structures based on apparent dextral offset of Paleogene strata. South of the map area, these faults exhibit normal offsets that partly define the edges of the basin in which the town of Yacolt is situated. North of these faults, the dominant fault trend in the quadrangle is northeasterly. The most prominent northeast-striking faults are those that control Chelatchie Prairie. Tertiary rocks that form the elongate knobs near Chelatchie strike almost north-south and appear to have been rotated several tens of degrees counterclockwise relative to strata that flank the basin. The knobs are interpreted as small blocks rotated along short subsidiary fault segments between longer left-lateral faults that transect and bound the basin. The basin itself evidently was formed by north-side-down normal offset on the faults that run along its southern boundary. Relief in this area is about 200 m but actual offset is unknown; it may be less than this because the basin was probably deepened by glacial erosion.

The age of the faulting is poorly constrained and movement may have occurred intermittently throughout late Cenozoic time. Zeolite- and quartz-filled fault planes and rusty pyritic rock in Cedar Creek south of Amboy presumably reflect reaction with heated geothermal fluids and indicate that some faulting probably occurred prior to the Miocene cessation of volcanic activity in the area. On the other hand, the major north-northwest and east-southeast striking fault zones are well expressed in the topography, suggesting that they are relatively young, possibly Quaternary structures. The relationship between these faults is unclear, but the north-northwest-striking faults that mark the abrupt west end of Chelatchie Prairie probably truncate the east-northeast faults. Chelatchie Prairie appears to be an oblique extensional feature formed in response to dextral motion on the north-northwest faults and associated clockwise rotation of the terrain to the west.

GEOLOGIC EVOLUTION

The late Eocene and early Oligocene bedrock in the Amboy quadrangle consists of sheetlike mafic to intermediate lava flows interbedded with coarse-grained breccias, pumiceous pyroclastic rocks, and stratified volcaniclastic sedimentary rocks and cut by scattered phaneritic intrusions. These bedrock units are typical of the

southern Washington Cascade Range (Evarts and Swanson, 1994). The dearth of dikes and areas of hydrothermal alteration in the map area suggests deposition largely in medial to distal settings beyond the flanks of large active volcanic edifices (Williams and McBirney, 1979; Vessell and Davies, 1981; Cas and Wright, 1987; Orton, 1996). Small silicic centers, however, may be marked by dacitic flows such as the one at Maple Pit, which are too viscous to flow far from source vents, and the wedge-like deposit of scoriaceous olivine-phyric basalt on the north flank of Green Mountain is probably a cross section through the flank of a small cinder cone. Also, the intrusions of diorite and quartz diorite at Buncombe Hollow, Dunegan Mountain and, elsewhere may represent subvolcanic magma chambers that fed now-eroded volcanoes. Age determinations in this and adjacent quadrangles (Evarts, 2002, 2004b; R.J. Fleck, written commun., 2000, 2001, 2002, 2005) show that the extrusive rocks here were emplaced mainly between 37 and 33 Ma, early in Cascade arc history (Duncan and Kulm, 1989; Evarts and Swanson, 1994). The uppermost unit in the map area, the basaltic andesite of Elkhorn Mountain, unconformably overlies the older strata and is about 27 m.y. old, indicating a hiatus in volcanism lasting perhaps as long as 6 m.y.; minor folding may have occurred during this time. Whether the event recorded by this hiatus was of regional or simply local extent is unknown, but generally the volcanic arc in Washington remained the site of vigorous volcanic activity into early Miocene time (Evarts and others, 1987; Vance and others, 1980; Smith, 1993). A precipitous decline in volcanism after about 17 Ma in southern Washington corresponds to a region-wide episode of uplift, folding, and erosion (Evarts and Swanson, 1994) and southward tilting of strata in the Amboy quadrangle probably occurred at this time.

Regionally distributed minor faults are believed to accommodate the deformation of crustal blocks that is recorded by clockwise-rotated paleomagnetic declinations in Paleogene rocks in southwestern Washington; this deformation is interpreted as a response to oblique convergence along the Cascadia Subduction Zone (Wells and Coe, 1985; Wells, 1989, 1990; Beck and Burr, 1979; Bates and others, 1981; Hagstrum and others, 1999). In the Amboy quadrangle, this deformation appears to have become concentrated along more discrete north-northwest- and east-northeast-trending fault zones. The NNW fault zone is most likely a dextral structure, one of a set along which western Washington has moved northward relative to interior North America (Wells and others, 1998). Chelatchie Prairie appears to be an extensional basin developed between antithetic oblique-slip faults with sinistral offset. It may have formed in a releasing stepover between the right-lateral fault zone near Amboy and a similar structure in the unmapped area east of the Amboy quadrangle; small blocks between the fault strands that bound Chelatchie Prairie have been rotated counterclockwise by left-lateral movement on these structures. The topographic expression of these faults suggests they are relatively young. The north-northwest-striking fault zone is parallel to the St. Helens Seismic Zone (SHZ) of Weaver and others (1987) beneath Mount St. Helens and thus is appropriately oriented for dextral strike-slip motion, as inferred for the SHZ, in the modern regional stress field (Pezzopane and Weldon, 1993; Wells and others, 1998; Miller and others, 2001).

The Quaternary geologic history recorded in the Amboy quadrangle reflects two dominating influences: Pleistocene glaciation and eruptions at the Mount St. Helens volcanic center, both of which caused alternating periods of alluviation and downcutting in the Lewis River valley in response to large variations in sediment load (Mundorff, 1984; Major and Scott, 1988). The modern topography owes much of its character to glacial sculpting.

Several times during the Pleistocene, mountain glaciers moved out of the Cascade Range and into the map area. Evidence for earlier glacial advances was erased by the glaciation that deposited the Amboy Drift, the local equivalent of the Hayden Creek Drift. During Amboy time, a large piedmont glacier issued from the Lewis River valley and spread out to bury the map area (Mundorff, 1984); at the glacier's maximum extent, only the summit of Green Mountain above about 1850 ft (565 m) projected above the ice. Evidence in the Ariel quadrangle (Evarts, 2004b) suggests that the Amboy Drift may include deposits of more than one glacial pulse during the Hayden Creek Stade, with the maximum advance occurring at about 270 ka. The most recent glaciation in the Cascade Range, which culminated about 17,000 ^{14}C years B.P. (Barnosky, 1984), was considerably less extensive than the Hayden Creek (Amboy) advance, and left no identified deposits in the lower Lewis River valley.

The Amboy-age glacier widened the valleys now occupied by Lake Merwin and Speelyai Creek and carved numerous streamlined knobs and ridges (rock drumlins) in the south part of the map area. The orientations of these features reflect the interplay between the west to south-southwest directions of ice movement and attitudes in the Paleogene bedrock; preferential excavation of volcaniclastic beds left elongated ridges upheld by lava flows. Prominent cuestas were produced in the south-dipping strata of Green Mountain and the ridge south of Speelyai Creek, and overdeepened troughs were carved in Chelatchie Prairie, Cedar Creek valley northwest of Amboy, and possibly the Lewis River valley. Glacial retreat was interrupted by multiple partial readvances, and proglacial drainage continually adjusted to changing position of ice margins. The bench now occupied by Buncombe Hollow Creek was probably eroded by a glacier-margin stream, as were several smaller drainages south of Chelatchie Prairie. Underfit streams such as Speelyai Creek, Chelatchie Creek, and Cedar Creek downstream from Amboy imply that significant rearrangements of stream courses took place during deglaciation. Mundorff (1984) suggested

that Canyon Creek, a large tributary that enters the Lewis River east of the map area, flowed approximately along the present course of Chelatchie Creek and westward along the modern Cedar Creek valley in preglacial times. The Lewis River may also have at times spilled into Chelatchie Prairie via the northeast-trending saddles north of Chelatchie. As the Amboy glacier retreated, proglacial outwash was deposited in the deglaciated valleys. Remnants of valley trains deposited when ice occupied Chelatchie Prairie are preserved as terraces along Cedar Creek and as a south-sloping fill in the Yacolt quadrangle to the south. The southwest-trending reach of Cedar Creek in the southeast part of the Amboy quadrangle probably drained southward to join the East Fork Lewis River at this time before being captured by headward erosion of lower Cedar Creek south of Amboy. Chelatchie Prairie itself filled with outwash when the glacier retreated farther upvalley.

The volcanic center at Mount St. Helens first became active at some time before or during the Amboy glaciation and has erupted frequently since (Crandell, 1987). At least one eruption occurred at a time when the Lewis River valley was filled with ice (Evarts, 2004b). Many of these eruptions were explosive, and some dumped huge quantities of pyroclastic debris into the Lewis River system. Evidence for periods of eruption-induced aggradation and subsequent incision is abundant in the Amboy quadrangle (Major and Scott, 1988). Most of the deposits of Mount St. Helens origin preserved within the quadrangle were deposited by lahars or reworked from primary eruptive deposits upstream. They postdate the Amboy Drift, and were largely deposited during the Ape Canyon, Cougar, and Swift Creek eruptive stages of Crandell (1987), between about 50,000 and 10,000 ^{14}C years B.P. (fig. 3) although younger deposits may underlie the submerged floodplain of the river. Thick fills of Mount St. Helens-derived debris in the valley of Speelyai Creek and the Lewis River valley east of Lake Merwin were probably emplaced during a major lahar-induced aggradational episode during the Cougar eruptive stage (Hyde, 1975; Major and Scott, 1988). Prior to Cougar time, the Lewis River may have flowed through the valley now occupied by Speelyai Creek, and was diverted southward to its present course when that valley became choked with volcaniclastic sediment, as suggested by Major and Scott (1988).

GEOLOGIC RESOURCES

Known geologic resources available in the Amboy quadrangle are limited to nonmetallic industrial materials, chiefly aggregate for road construction and similar purposes. Several large quarries in Paleogene volcanic and intrusive bedrock of the map area produce crushed aggregate used primarily as base and surface material for roads. Sand and gravel are locally available from unconsolidated alluvial deposits along the Lewis River but are more abundant and accessible downstream from the map area.

REFERENCES CITED

Balsillie, J.H., and Benson, G.T., 1971, Evidence for the Portland Hills Fault: The Ore Bin, v. 33, p. 109–118.

Barnosky, C.W., 1984, Late Pleistocene and early Holocene environmental history of southwestern Washington State, U.S.A.: Canadian Journal of Earth Sciences, v. 21, p. 619–629.

Bates, R.G., Beck, M.E., Jr., and Burmester, R.F., 1981, Tectonic rotations in the Cascade Range of southern Washington: Geology, v. 9, p. 184–189.

Beck, M.E., Jr., and Burr, C.D., 1979, Paleomagnetism and tectonic significance of the Goble Volcanic Series, southwestern Washington: Geology, v. 7, p. 175–179.

Beeson, M.H., Fecht, K.R., Reidel, S.P., and Tolan, T.L., 1985, Regional correlations within the Frenchman Springs Member of the Columbia River Basalt Group—new insights into the middle Miocene tectonics of northwestern Oregon: Oregon Geology, v. 47, p. 87–96.

Beeson, M.H., Tolan, T.L., and Anderson, J.L., 1989, The Columbia River Basalt Group in western Oregon—geologic structures and other factors that controlled flow emplacement patterns, *in* Reidel, S.P., and Hooper, P.R, eds., Volcanism and tectonism in the Columbia River flood-basalt province: Geological Society of America Special Paper 239, p. 223–246.

Berger, G.W., and Busacca, A.J., 1995, Thermoluminescence dating of late Pleistocene loess and tephra from eastern Washington and southern Oregon and implications for the eruptive history of Mount St. Helens: Journal of Geophysical Research, v. 100, p. 22361–22374.

Berggren, W.A., Kent, D.V., Swisher, C., III, Aubry, M.-P., 1995, A revised Cenozoic geochronology and chronostratigraphy, *in* Berggren, W.A., Kent, D.V., Aubry, M.-P., and Hardenbol, Jan, eds., Geochronology, time scales and global stratigraphic correlation: Society of Economic Paleontologists and Mineralogists Special Publication 54, p. 129–212.

Blakely, R.J., Wells, R.E., Yelin, T.S., Madin, I.P., and Beeson, M.H., 1995, Tectonic setting of the Portland-Vancouver area, Oregon and Washington—constraints from low-altitude aeromagnetic data: Geological Society of America Bulletin, v. 107, p. 1051–1062.

Bott, J.D.J., and Wong, I.G., 1993, Historical earthquakes in and around Portland, Oregon: Oregon Geology, v. 55, p. 116–122.

Cas, R.A.F., and Wright, J.V., 1987, Volcanic successions—modern and ancient: London, Allen and Unwin, 528 p.

Cho, M., Maruyama, S., and Liou, J.G., 1987, An experimental investigation of heulandite-laumontite equilibrium at 1000 to 2000 bar P_{fluid}: Contributions to Mineralogy and Petrology, v. 97, p. 43–50.

Colman, S.M., and Pierce, K.L., 1981, Weathering rinds on andesitic and basaltic stones as a Quaternary age indicator, western United States: U.S. Geological Survey Professional Paper 1210, 56 p.

Crandell, D.R., 1987, Deposits of pre-1980 pyroclastic flows and lahars from Mount St. Helens, Washington: U.S. Geological Survey Professional Paper 1444, 91 p.

Crandell, D.R., and Miller, R.D., 1974, Quaternary stratigraphy and extent of glaciation in the Mount Rainier region, Washington: U.S. Geological Survey Professional Paper 847, 59 p.

Dethier, D.P., 1988, The soil chronosequence along the Cowlitz River, Washington: U.S. Geological Survey Bulletin 1590-F, p. F1–F47.

Duncan, R.A., and Kulm, L.D., 1989, Plate tectonic evolution of the Cascades arc-subduction complex, *in* Winterer, E.L., Hussong, D.M., and Decker, R.W., eds., The eastern Pacific Ocean and Hawaii: Boulder, Colo., Geological Society of America, The geology of North America, v. N, p. 413–438.

Evarts, R.C., 2001, Geologic map of the Silver Lake quadrangle, Cowlitz County, Washington: U.S. Geological Survey Miscellaneous Field Studies Map MF-2371, scale 1:24,000, with 37-p. pamphlet [Available on the World Wide Web at http://pubs.usgs.gov/mf/2001/2371/].

Evarts, R.C., 2002, Geologic map of the Deer Island quadrangle, Cowlitz County, Washington: U.S. Geological Survey Miscellaneous Field Studies Map MF-2392, scale 1:24,000, with 33-p. pamphlet [Available on the World Wide Web at http://pubs.usgs.gov/mf/2002/2392/].

Evarts, R.C., 2004a, Geologic map of the Woodland quadrangle, Cowlitz and Clark Counties, Washington: U.S. Geological Survey Scientific Investigations Map 2827, scale 1:24,000, with 38-p. pamphlet [Available on the World Wide Web at http://pubs.usgs.gov/sim/2004/2827].

Evarts, R.C., 2004b, Geologic map of the Ariel quadrangle, Clark and Cowlitz Counties, Washington: U.S. Geological Survey Scientific Investigations Map 2826, scale 1:24,000, with 35-p. pamphlet [Available on the World Wide Web at http://pubs.usgs.gov/sim/2004/2826].

Evarts, R.C., and Ashley, R.P., 1990a, Preliminary geologic map of the Cougar quadrangle, Cowlitz and Clark Counties, Washington: U.S. Geological Survey Open-File Report 90-631, scale 1:24,000, with 40-p. pamphlet.

Evarts, R.C., and Ashley, R.P., 1990b, Preliminary geologic map of the Goat Mountain quadrangle, Cowlitz County, Washington: U.S. Geological Survey Open-File Report 90-632, scale 1:24,000, with 47-p. pamphlet.

Evarts, R.C., and Ashley, R.P., 1991, Preliminary geologic map of the Lakeview Peak quadrangle, Cowlitz County, Washington: U.S. Geological Survey Open-File Report 91-289, scale 1:24,000, with 35-p. pamphlet.

Evarts, R.C., and Ashley, R.P., 1992, Preliminary geologic map of the Elk Mountain quadrangle, Cowlitz County, Washington: U.S. Geological Survey Open-File Report 92-362, scale 1:24,000, with 44-p. pamphlet.

Evarts, R.C., Ashley, R.P., and Smith, J.G., 1987, Geology of the Mount St. Helens area—record of discontinuous volcanic and plutonic activity in the Cascade arc of southern Washington: Journal of Geophysical Research, v. 92, p. 10,155–10,169.

Evarts, R.C., and Bishop, K.R., 1994, Chemical data for Tertiary volcanic and intrusive rocks of the Spirit Lake 15-minute quadrangle, southern Washington Cascade Range: U.S. Geological Survey Open-File Report 93-686, 24 p.

Evarts, R.C., Clynne, M.A., Fleck, R.J., Lanphere, M.A., Calvert, A.T., and Sarna-Wojcicki, A.M., 2003, The antiquity of Mount St. Helens and age of the Hayden Creek Drift [abs.]: Geological Society of America Abstracts with program, v. 35, no. 6, p. 80.

Evarts, R.C., and Swanson, D.A., 1994, Geologic transect across the Tertiary Cascade Range, southern Washington, *in* Swanson, D.A., Haugerud, R.A., eds., Geologic field trips in the Pacific Northwest, 1994 Geological Society of America Meeting: Seattle, University of Washington Department of Geological Sciences, v. 2, p. 2H1–2H31.

Fiksdal, A.J., 1975, Slope stability of Clark County, Washington: Washington Division of Geology and Earth Resources Open-File Report 75-10, scale 1:62,500, with 4-p. pamphlet.

Fiske, R.S., Hopson, C.A., and Waters, A.C., 1963, Geology of Mount Rainier National Park, Washington: U.S. Geological Survey Professional Paper 444, 93 p.

Gill, J.B., 1981, Orogenic andesites and plate tectonics: New York, Springer-Verlag, 390 p.

Grigg, L.D., and Whitlock, C., 2002, Patterns and causes of millennial-scale climate change in the Pacific Northwest during Marine Isotope stages 2 and 3: Quaternary Science Reviews, v. 21, p. 2067–2083.

Hagstrum, J.T., Swanson, D.A., and Evarts, R.C., 1999, Paleomagnetism of an east-west transect across the Cascade arc in southern Washington—implications for regional tectonism: Journal of Geophysical Research, v. 104, p. 12853–12864.

Howard, K.A., 2002, Geologic map of the Battle Ground 7.5-minute quadrangle, Clark County, Washington: U.S. Geological Survey Miscellaneous Field Studies Map MF-2395, scale 1:24,000, with 18-p. pamphlet.

Hyde, J.H., 1975, Upper Pleistocene pyroclastic-flow deposits and lahars south of Mount St. Helens volcano, Washington: U.S. Geological Survey Bulletin 1383-B, 20 p.

Johnson, D.M., Hooper, P.R., and Conrey, R.M., 1999, XRF analysis of rocks and minerals for major and trace elements on a single low dilution Li-tetraborate fused bead: Advances in X-ray Analysis, v. 41, p. 843–867.

Le Maitre, R.W., 2002, Igneous rocks—a classification and glossary of terms, 2d ed.: Cambridge University Press, 236 p.

Liberty, L.M., Hemphill-Haley, M.A., and Madin, I.P., 2003, The Portland Hills Fault—uncovering a hidden fault in Portland, Oregon using high-resolution geophysical methods: Tectonophysics, v. 368, p. 89–103.

Madin, I.P., Wang, Z., 1999, Relative earthquake hazard maps for selected urban areas in western Oregon–Dallas, Hood River, McMinnville-Dayton-Lafayette, Monmouth-Independence, Newberg-Dundee, Sandy, Sheridan-Willamina, Saint Helens-Columbia City-Scappoose: Oregon Department of Geology and Mineral Industries Interpretive Map Series Map IMS-7, scale 1:24,000, with 24-p. pamphlet.

Major, J.J., and Scott, K.M., 1988, Volcaniclastic sedimentation in the Lewis River valley, Mount St. Helens, Washington—processes, extent, and hazards: U.S. Geological Survey Bulletin 1383-D, 38 p.

Martinson, D.G., Pisias, N.G., Hayes, J.D., Imbrie, J., Moore, T.C., Jr., and Shackleton, N.J., 1987, Age dating and orbital theory of the ice ages—development of a high-resolution 0 to 300,000-year chronostratigraphy: Quaternary Research, v. 27, p. 1–29.

Miller, M.M., Johnson, D.J., Rubin, C.M., Dragert, H., Wang, K., Qamar, A., and Goldfinger, C., 2001, GPS-determination of along-strike variation in Cascadia margin kinematics—implications for relative plate motion, subduction zone coupling, and permanent deformation: Tectonics, v. 20, p. 161–171.

Miyashiro, A., 1974, Volcanic rocks series in island arcs and active continental margins: American Journal of Science, v. 274, p. 321–355.

Mullineaux, D.R., 1996, Pre-1980 tephra-fall deposits erupted from Mount St. Helens: U.S. Geological Survey Professional Paper 1563, 99 p.

Mundorff, M.J., 1964, Geology and ground-water conditions of Clark County, Washington, with a description of a major alluvial aquifer along the Columbia River: U.S. Geological Survey Water-Supply Paper 1600, 268 p., scale 1:48,000.

Mundorff, M.J., 1984, Glaciation in the lower Lewis River basin, southwestern Cascade Range, Washington: Northwest Science, v. 58, p. 269–281.

Orton, G.J., 1996, Volcanic environments, *in* Reading, H.G., ed., Sedimentary environments—processes, facies and stratigraphy, (3d ed.): Oxford, Blackwell Science, Ltd., p. 485–567.

Pezzopane, S.K., and Weldon, R.J., II, 1993, Tectonic role of active faulting in central Oregon: Tectonics, v. 12, p. 1140–1169.

Phillips, W.M., 1987, comp., Geologic map of the Vancouver quadrangle, Washington: Washington Division of Geology and Earth Resources Open-File Report 87-10, scale 1:100,000, with 27-p. pamphlet.

Roberts, A.E., 1958, Geology and coal resources of the Toledo-Castle Rock district, Cowlitz and Lewis Counties, Washington: U.S. Geological Survey Bulletin 1062, 71 p.

Smith, G.A., 1986, Coarse-grained nonmarine volcaniclastic sediment—terminology and depositional processes: Geological Society of America Bulletin, v. 97, p. 1–10.

Smith, J.G., 1993, Geologic map of upper Eocene to Holocene volcanic and related rocks in the Cascade Range, Washington: U.S. Geological Survey Miscellaneous Investigation Series Map I-2005, scale 1:500,000.

Snavely, P.D., Jr., Brown, R.D., Jr., Roberts, A.E., and Rau, W.W., 1958, Geology and coal resources of the Centralia-Chehalis district, Washington: U.S. Geological Survey Bulletin 1053, 159 p.

Swanson, R.D., McFarland, W.D., Gonthier, J.B., and Wilkinson, J.M., 1993, A description of hydrogeologic units in the Portland Basin, Oregon and Washington: U.S. Geological Survey Water-Resources Investigations Report 90-4196, 56 p., scale 1:100,000.

Trimble, D.E., 1963, Geology of Portland, Oregon and adjacent areas: U.S. Geological Survey Bulletin 1119, 119 p., scale 1:62,500.

Vance, J.A., Clayton, G.A., Mattinson, J.M., and Naeser, C.W., 1987, Early and middle Cenozoic stratigraphy of the Mount Rainier-Tieton River area, southern Washington Cascades, *in* Schuster, E.J., ed., Selected papers on the geology of Washington: Washington Division of Geology and Earth Resources Bulletin 77, p. 269-290.

Vessell, R.K., and Davies, D.K., 1981, Nonmarine sedimentation in an active fore arc basin, *in* Ethridge, F.G., and Flores, R.M., eds., Recent and ancient nonmarine depositional environments—models for exploration: Society of Economic Paleontologists and Mineralogists Special Publication 31, p. 31–45.

Walsh, T.J., Korosec, M.A., Phillips, W.M., Logan, R.L., and Schasse, H.W., 1987, Geologic map of Washington—southwest quadrant: Washington Division of Geology and Earth Resources Map GM-34, scale 1:250,000.

Weaver, C.S., Grant, W.C., and Shemeta, J.E., 1987, Local crustal extension at Mount St. Helens, Washington: Journal of Geophysical Research, v. 93, p. 10,170–10,178.

Wegmann, K.W., and Walsh, T.J., 2001, Landslide hazards mapping in Cowlitz County—a progress report: Washington Geology, v. 29, no. 1/2, p. 30–33.

Wells, R.E., 1981, Geologic map of the eastern Willapa Hills, Cowlitz, Lewis, Pacific, and Wahkiakum Counties, Washington: U.S. Geological Survey Open-File Report 81-674, scale 1:62,500.

Wells, R.E., 1989, Mechanisms of Cenozoic tectonic rotation, Pacific Northwest convergent margin, U.S.A., *in* Kissel, C., and Laj, C., eds., Paleomagnetic rotations and continental deformation: Dordrecht, Kluwer Academic Publishers, p. 313–325.

Wells, R.E., 1990, Paleomagnetic rotations and the Cenozoic tectonics of the Cascade arc, Washington, Oregon, and California: Journal of Geophysical Research, v. 95, p. 19,409–19,417.

Wells, R.E., and Coe, R.S., 1985, Paleomagnetism and geology of Eocene volcanic rocks of southwest Washington, implications for mechanisms of tectonic rotation: Journal of Geophysical Research, v. 90, p. 1925–1947.

Wells, R.E., Weaver, C.S., and Blakely, R.J., 1998, Fore-arc migration in Cascadia and its neotectonic significance: Geology, v. 26, p. 759–762.

Whitlock, C., Sarna-Wojcicki, A.M., Bartlein, P.J., and Nickmann, R.J., 2000, Environmental history and tephrostratigraphy at Carp Lake, southwestern Columbia Basin, USA: Paleogeography, Paleoclimatology, Paleoecology, v. 155, p. 7–29.

Wilkinson, W.D., Lowry, W.D., and Baldwin, E.M., 1946, Geology of the St. Helens quadrangle, Oregon: Oregon Department of Geology and Mineral Industries Bulletin 31, scale 1:62,500, 39 p.

Williams, H., and McBirney, A.R., 1979, Volcanology: San Francisco, Freeman, Cooper and Co., 397 p.

Wise, W.S., 1970, Cenozoic volcanism in the Cascade Mountains of southern Washington: Washington Division of Mines and Geology Bulletin 60, 45 p.

Wong, I.G., Hemphill-Haley, A., Liberty, L.M., and Madin, I.P., 2001, The Portland Hills Fault—an earthquake generator or just another old fault?: Oregon Geology, v. 63, p. 39–50.

Yelin, T.S., and Patton, H.J., 1991, Seismotectonics of the Portland, Oregon, region: Seismological Society of America Bulletin, v. 81, p. 109–130.

Table 1. Chemical analyses of volcanic and intrusive rocks, Amboy 7.5' quadrangle

[X-ray fluorescence analyses. Rock-type names assigned in accordance with IUGS system (Le Maitre, 2002) applied to recalculated analyses. FeO*, total iron calculated as FeO. Mg#, atomic ratio 100Mg/(Mg+Fe^{2+}) with Fe^{2+} set to 0.85x Fe^{total}. Modal analyses, secondary minerals counted as primary mineral replaced. -, not present. X-ray fluorescence analyses by D.M. Johnson at GeoAnalytical Laboratory of Washington State University using methods described in Johnson and others (1999)]

Map No.	1	2	3	4	5	6	7	8	9
Field sample No.	**02YC-P466**	**99YC-P68**	**99YC-P41A**	**99YC-P58**	**99YC-P95A**	**99YC-P59**	**00YC-P129C**	**00YC-P210**	**00YC-P164**
Latitude (N)	45°57.94'	45°57.84'	45°59.46'	45°59.10'	45°57.84'	45°57.10'	45°53.76'	45°53.52'	45°52.86'
Longitude (W)	122°25.19'	122°27.12'	122°28.02'	122°23.34'	122°27.30'	122°22.80'	122°23.22'	122°23.40'	122°22.86'
Map unit	Tob	Tob	Tb	Tb	Tb	Tppb	Tbem	Tbem	Tbem
Rock type	Basalt	Basaltic andesite	Basalt	Basalt	Basalt	Basalt	Basaltic andesite	Basaltic andesite	Basaltic andesite
Analyses as reported (wt percent)									
SiO_2	47.34	52.62	51.16	51.25	51.74	50.58	52.16	52.46	53.33
TiO_2	1.78	1.28	1.74	1.78	1.33	1.61	1.24	1.39	1.36
Al_2O_3	15.53	16.53	15.35	15.33	17.30	16.35	19.39	17.87	17.25
FeO*	9.93	8.90	10.68	10.83	8.49	10.20	8.63	9.69	9.60
MnO	0.17	0.15	0.19	0.21	0.17	0.18	0.16	0.18	0.17
MgO	9.48	7.11	5.66	5.59	6.62	5.30	4.33	4.42	4.44
CaO	10.30	9.54	10.26	10.09	9.71	10.67	10.74	9.63	9.85
Na_2O	2.59	2.91	3.28	3.29	3.15	3.00	2.91	3.06	2.97
K_2O	0.97	0.70	0.49	0.49	0.88	0.45	0.38	0.48	0.78
P_2O_5	0.47	0.27	0.24	0.25	0.28	0.21	0.16	0.19	0.19
Total	98.56	100.01	99.05	99.11	99.67	98.55	100.10	99.37	99.94
Analyses recalculated volatile-free and normalized to 100% with all Fe as FeO (wt percent)									
SiO_2	48.03	52.61	51.65	51.71	51.91	51.32	52.11	52.79	53.36
TiO_2	1.81	1.28	1.76	1.80	1.33	1.63	1.24	1.40	1.36
Al_2O_3	15.76	16.53	15.50	15.47	17.36	16.59	19.37	17.98	17.26
FeO*	10.08	8.90	10.78	10.93	8.52	10.35	8.62	9.75	9.61
MnO	0.17	0.15	0.19	0.21	0.17	0.18	0.16	0.18	0.17
MgO	9.62	7.11	5.71	5.64	6.64	5.38	4.33	4.45	4.44
CaO	10.45	9.54	10.36	10.18	9.74	10.83	10.73	9.69	9.86
Na_2O	2.63	2.91	3.31	3.32	3.16	3.04	2.91	3.08	2.97
K_2O	0.98	0.70	0.49	0.49	0.88	0.46	0.38	0.48	0.78
P_2O_5	0.48	0.27	0.24	0.25	0.28	0.21	0.16	0.19	0.19
Mg#	66.7	62.6	52.6	52.0	62.1	52.1	51.3	48.9	49.2
Modes (volume percent)									
Plagioclase	-	0.3	-	-	1.1	16.2	26.8	21.9	14.0
Clinopyroxene	-	0.1	-	-	0.2	-	trace	0.3	1.3
Orthopyroxene	-	-	-	-	-	-	-	-	-
Olivine	9.3	7.0	-	-	2.3	0.3	0.1	2.8	0.6
Fe-Ti Oxide	-	-	-	-	trace	-	-	-	-
Hornblende	-	-	-	-	-	-	-	-	-
Quartz	-	-	-	-	-	-	-	-	-
K-feldspar	-	-	-	-	-	-	-	-	-
Other	-	-	-	-	-	-	-	-	-
Groundmass	90.7	92.6	100.0	100.0	96.4	83.5	73.1	75.0	84.1
No. points counted	788	718			726	750	800	795	766
Texture (rock/ groundmass)	porphyritic/ trachytic	porphyritic/ trachytic	aphyric/ intergranular	aphyric/ intergranular	sparsely phyric/ trachytic	porphyritic/ intergranular	porphyritic/ trachytic	seriate/ trachytic	seriate/ microgranular
Trace element analyses (ppm)									
Ba	264	161	125	126	169	102	134	137	173
Rb	23	7	8	5	14	3	4	5	23
Sr	410	435	270	262	431	283	341	311	289
Y	23	22	32	34	23	29	21	25	30
Zr	177	145	123	129	144	113	95	100	132
Nb	16.4	10.7	9.9	10.0	11.7	9.2	5.9	7.1	8.8
Ni	193	149	28	32	97	38	20	11	13
Cu	100	133	151	151	114	141	125	152	165
Zn	80	80	88	90	78	87	73	81	75
Cr	403	258	66	67	155	70	45	48	52

Table 1. Chemical analyses of volcanic and intrusive rocks, Amboy 7.5' quadrangle—Continued

Map No.	10	11	12	13	14	15	16	17	18
Field sample No.	**00YC-P128A**	**00YC-P167**	**00YC-P98**	**00YC-P101**	**00YC-P209**	**01YC-P230**	**01YC-P215B**	**01YC-P225**	**01YC-P215A**
Latitude (N)	45°54.00'	45°52.62'	45°53.10'	45°54.12'	45°52.92'	45°53.10'	45°53.04'	45°52.98'	45°53.10'
Longitude (W)	122°22.50'	122°22.62'	122°27.72'	122°24.30'	122°23.58'	122°26.58'	122°28.74'	122°29.22'	122°28.74'
Map unit	Tbem	Tbem	Tbem	Tbem	Tbem	Tbem	Tbem	Tbem	Tbem
Rock type	Basaltic andesite	Basaltic andesite	Basaltic andesite	Basaltic andesite	Basaltic andesite	Basaltic andesite	Basaltic andesite	Basaltic andesite	Basaltic andesite
Analyses as reported (wt percent)									
SiO_2	53.52	53.73	54.74	54.89	55.43	55.02	55.20	55.23	56.16
TiO_2	1.67	1.67	1.16	1.20	1.22	1.12	1.12	1.18	1.59
Al_2O_3	15.92	16.15	20.12	19.08	17.68	19.58	19.37	19.13	16.37
FeO*	10.33	10.14	7.20	7.87	8.91	7.24	7.49	7.35	9.70
MnO	0.20	0.18	0.15	0.16	0.17	0.16	0.18	0.18	0.21
MgO	4.63	4.58	2.68	3.10	4.16	2.66	2.65	2.58	3.18
CaO	9.42	9.32	9.44	8.79	8.49	8.91	8.76	8.67	7.46
Na_2O	2.97	3.11	3.46	3.44	3.43	3.67	3.65	3.62	4.01
K_2O	0.54	0.69	0.52	0.58	0.54	0.60	0.62	0.65	0.70
P_2O_5	0.24	0.24	0.19	0.19	0.17	0.18	0.18	0.18	0.23
Total	99.44	99.81	99.66	99.30	100.20	99.14	99.22	98.77	99.61
Analyses recalculated volatile-free and normalized to 100% with all Fe as FeO (wt percent)									
SiO_2	53.82	53.83	54.93	55.28	55.32	55.50	55.64	55.92	56.38
TiO_2	1.68	1.67	1.17	1.21	1.22	1.13	1.13	1.19	1.60
Al_2O_3	16.01	16.18	20.19	19.22	17.65	19.75	19.52	19.37	16.43
FeO*	10.39	10.16	7.23	7.93	8.89	7.30	7.55	7.44	9.74
MnO	0.20	0.18	0.15	0.16	0.17	0.16	0.18	0.18	0.21
MgO	4.66	4.59	2.69	3.12	4.15	2.68	2.67	2.61	3.19
CaO	9.47	9.34	9.47	8.85	8.47	8.99	8.83	8.78	7.49
Na_2O	2.99	3.12	3.47	3.46	3.42	3.70	3.68	3.67	4.03
K_2O	0.54	0.69	0.52	0.58	0.54	0.61	0.62	0.66	0.70
P_2O_5	0.24	0.24	0.19	0.19	0.17	0.18	0.18	0.18	0.23
Mg#	48.4	48.6	43.8	45.3	49.5	43.5	42.6	42.4	40.7
Modes (volume percent)									
Plagioclase	3.7	3.5	40.9	44.3	28.3	29.8	28.5	8.5	8.5
Clinopyroxene	-	-	1.1	1.8	0.4	0.9	1.6	1.5	1.5
Orthopyroxene	-	-	-	-	1.5	-	-	-	-
Olivine	0.6	0.3	0.7	2.6	0.2	1.3	1.0	0.6	0.6
Fe-Ti Oxide	-	-	0.1	0.2	trace	0.1	0.4	0.3	0.3
Hornblende	-	-	-	-	-	-	-	-	-
Quartz	-	-	-	-	-	-	-	-	-
K-feldspar	-	-	-	-	-	-	-	-	-
Other	-	-	-	-	-	-	-	-	-
Groundmass	95.7	96.2	57.2	51.1	69.6	67.9	68.5	89.1	89.1
No. points counted	771	733	736	810	792	775	796	786	786
Texture (rock/ groundmass)	seriate/ trachytic	seriate/ trachytic	seriate/ intergranular	porphyritic/ intergranular	seriate/ intergranular	seriate/ intergranular	seriate/ intergranular	seriate/ intergranular	seriate/ intergranular
Trace element analyses (ppm)									
Ba	200	219	143	155	155	151	154	147	147
Rb	8	14	8	11	8	11	14	16	16
Sr	280	275	334	320	326	325	324	272	272
Y	31	31	26	25	23	24	29	33	33
Zr	140	142	108	115	93	112	111	135	135
Nb	8.2	9.0	8.7	8.6	6.8	8.8	8.3	10.5	10.5
Ni	20	16	3	8	12	2	3	3	3
Cu	221	174	49	94	107	114	107	171	171
Zn	90	94	72	79	76	78	75	103	103
Cr	54	55	9	20	36	10	12	10	10

Table 1. Chemical analyses of volcanic and intrusive rocks, Amboy 7.5' quadrangle—Continued

Map No.	19	20	21	22	23	24	25	26	27
Field sample No.	**00YC-P131A**	**01YC-P288**	**99YC-P61**	**01YC-P293**	**01YC-P351**	**99YC-P54**	**99YC-P29**	**99YC-P22**†	**99YC-P88**
Latitude (N)	45°55.80'	45°58.44'	45°58.02'	45°58.56'	45°52.62'	45°58.92'	45°53.64'	45°59.58'	45°57.06'
Longitude (W)	122°26.40'	122°24.06'	122°29.82'	122°23.88'	122°24.60'	122°23.58'	122°29.76'	122°25.02'	122°27.18'
Map unit	Tbem	Tba	Tba	Tba	Tba	Tba	Tba	Tba	Tba
Rock type	Basaltic andesite	Basaltic andesite	Basaltic andesite	Basaltic andesite	Basaltic andesite	Basaltic andesite	Basaltic andesite	Basaltic andesite	Basaltic andesite
Analyses as reported (wt percent)									
SiO_2	52.20	52.27	53.43	53.51	53.46	53.82	54.16	54.05	54.61
TiO_2	1.61	0.98	0.90	2.11	1.09	2.13	0.94	1.70	1.15
Al_2O_3	16.96	20.45	18.79	15.79	18.37	15.51	17.77	18.08	17.38
FeO*	9.16	7.72	7.19	10.47	8.32	11.15	8.09	8.01	7.97
MnO	0.16	0.15	0.14	0.22	0.18	0.17	0.15	0.13	0.30
MgO	4.69	3.60	5.17	4.17	4.53	3.61	4.92	3.28	4.72
CaO	9.86	10.15	9.95	8.12	9.55	8.01	9.44	8.29	9.67
Na_2O	2.98	3.21	3.08	3.93	3.15	3.87	2.97	3.96	3.16
K_2O	1.23	0.57	0.75	0.84	0.52	0.77	0.71	1.04	0.71
P_2O_5	0.30	0.14	0.13	0.37	0.15	0.34	0.14	0.35	0.19
Total	99.15	99.24	99.53	99.53	99.32	99.38	99.29	98.89	99.86
Analyses recalculated volatile-free and normalized to 100% with all Fe as FeO (wt percent)									
SiO_2	52.65	52.67	53.68	53.76	53.82	54.16	54.55	54.66	54.72
TiO_2	1.62	0.99	0.90	2.12	1.10	2.14	0.95	1.72	1.32
Al_2O_3	17.11	20.61	18.88	15.87	18.50	15.61	17.90	18.28	16.96
FeO*	9.24	7.78	7.22	10.52	8.38	11.22	8.15	8.10	8.03
MnO	0.16	0.16	0.14	0.22	0.19	0.17	0.15	0.13	0.15
MgO	4.73	3.63	5.19	4.19	4.56	3.63	4.96	3.32	5.57
CaO	9.94	10.23	10.00	8.16	9.61	8.06	9.51	8.38	8.90
Na_2O	3.01	3.23	3.09	3.95	3.17	3.89	2.99	4.00	3.43
K_2O	1.24	0.57	0.75	0.84	0.52	0.77	0.72	1.05	0.65
P_2O_5	0.30	0.14	0.13	0.37	0.15	0.35	0.14	0.35	0.28
Mg#	51.8	49.4	60.1	45.5	53.3	40.4	56.0	46.2	59.3
Modes (volume percent)									
Plagioclase	14.4	37.6	16.3	-	29.6	-	26.5	38.7	10.1
Clinopyroxene	1.9	-	-	-	0.8	-	4.7	-	0.8
Orthopyroxene	-	-	-	-	0.1	-	0.5	0.3	0.4
Olivine	2.2	0.3	1.6	-	3.6	-	2.8	0.5	1.4
Fe-Ti Oxide	0.1	-	-	-	-	-	-	-	0.4
Hornblende	-	-	-	-	-	-	-	-	-
Quartz	-	-	-	-	-	-	-	-	-
K-feldspar	-	-	-	-	-	-	-	-	-
Other	-	-	-	-	-	-	-	-	-
Groundmass	81.4	62.1	82.1	100.0	65.9	100.0	65.5	60.5	86.9
No. points counted	742	747	774		753		784	782	760
Texture (rock/ groundmass)	porphyritic/ trachytic	porphyritic/ intergranular	seriate/ intergranular	aphyric/ trachytic	seriate/ intergranular	aphyric/ intersertal	seriate/ intergranular	porphyritic/ intergranular	seriate/ intergranular
Trace element analyses (ppm)									
Ba	563	141	139	203	121	194	137	224	212
Rb	18	12	13	12	10	11	13	15	9
Sr	599	312	397	363	292	404	322	404	378
Y	33	20	18	31	22	33	18	32	24
Zr	179	91	111	155	97	156	100	198	167
Nb	10.2	6.1	7.2	13.7	6.6	12.6	5.6	16.5	13.6
Ni	36	14	49	10	16	3	28	35	64
Cu	77	94	43	140	63	39	88	99	100
Zn	85	73	61	98	84	104	73	89	71
Cr	56	20	106	16	35	19	67	49	110

† float

Table 1. Chemical analyses of volcanic and intrusive rocks, Amboy 7.5' quadrangle—Continued

Map No.	28	29	30	31	32	33	34	35	36
Field sample No.	**98YC-P09**	**99YC-P35**	**99YC-P11A**	**00YC-P171**	**98YC-P04**	**83YC-P01E**	**99YC-P93**	**99YC-P86**	**99YC-P82A**
Latitude (N) Longitude (W)	45°58.98' 122°26.52'	45°57.42' 122°28.68'	45°55.98' 122°22.68'	45°55.08' 122°22.86'	45°59.28' 122°26.16'	45°59.28' 122°25.14'	45°57.90' 122°28.32'	45°55.74' 122°28.74'	45°56.28' 122°25.32'
Map unit	Tba	Tba	Tba	Tba	Tba	Tiba	Tba	Tba	Tba
Rock type	Basaltic andesite	Basaltic andesite	Basaltic andesite	Basaltic andesite	Basaltic andesite	Basaltic andesite	Basaltic andesite	Basaltic andesite	Basaltic andesite
Analyses as reported (wt percent)									
SiO_2	54.08	54.71	54.66	54.44	54.38	54.63	55.48	55.51	55.47
TiO_2	2.20	1.05	1.31	1.23	2.23	2.01	1.07	1.78	1.60
Al_2O_3	15.68	17.57	17.89	17.71	15.66	15.36	18.07	15.72	16.09
FeO*	10.11	8.01	8.77	8.38	10.30	9.72	7.75	9.91	9.45
MnO	0.20	0.15	0.16	0.16	0.19	0.17	0.15	0.21	0.16
MgO	3.45	4.49	3.46	4.19	3.27	4.32	4.42	3.92	3.96
CaO	6.93	9.42	8.80	8.56	6.85	8.41	9.12	7.57	7.66
Na_2O	4.44	3.34	3.28	3.50	4.35	3.65	3.40	3.79	3.78
K_2O	1.02	0.76	0.83	0.58	1.04	0.59	0.75	0.89	0.88
P_2O_5	0.53	0.16	0.21	0.19	0.53	0.38	0.17	0.26	0.26
Total	98.64	99.66	99.37	98.94	98.80	99.24	100.38	99.56	99.31
Analyses recalculated volatile-free and normalized to 100% with all Fe as FeO (wt percent)									
SiO_2	54.83	54.90	55.01	55.03	55.04	55.05	55.27	55.76	55.86
TiO_2	2.23	1.06	1.32	1.24	2.26	2.03	1.07	1.78	1.61
Al_2O_3	15.90	17.63	18.00	17.90	15.85	15.48	18.00	15.79	16.20
FeO*	10.25	8.04	8.82	8.47	10.43	9.79	7.72	9.96	9.52
MnO	0.21	0.15	0.16	0.16	0.19	0.17	0.15	0.21	0.16
MgO	3.50	4.51	3.48	4.24	3.31	4.35	4.40	3.94	3.99
CaO	7.03	9.45	8.86	8.65	6.93	8.47	9.09	7.60	7.71
Na_2O	4.50	3.35	3.30	3.54	4.40	3.68	3.39	3.81	3.81
K_2O	1.03	0.76	0.84	0.59	1.05	0.59	0.75	0.89	0.89
P_2O_5	0.53	0.16	0.21	0.19	0.54	0.38	0.17	0.26	0.26
Mg#	41.7	54.0	45.3	51.2	40.0	48.3	54.5	45.3	46.8
Modes (volume percent)									
Plagioclase	-	7.6	24.2	31.1	trace	0.6	9.2	1.0	0.2
Clinopyroxene	-	0.3	1.8	1.6	-	trace	0.1	0.1	trace
Orthopyroxene	-	-	-	2.1	-	-	-	-	-
Olivine	-	0.4	1.5	1.3	-	trace	0.3	-	-
Fe-Ti Oxide	-	-	trace	0.4	-	-	-	-	-
Hornblende	-	-	-	-	-	-	-	-	-
Quartz	-	-	-	-	-	-	-	-	-
K-feldspar	-	-	-	-	-	-	-	-	-
Other	-	-	-	-	-	-	-	-	-
Groundmass	100.0	91.7	72.5	63.5	100.0	99.4	90.4	98.9	99.8
No. points counted		753	792	792		802	802	800	750
Texture (rock/ groundmass)	aphyric/ trachytic	seriate/ microgranular	seriate/ intersertal	seriate/ intersertal	aphyric/ trachytic	sparsely phyric/ intersertal	seriate/ intergranular	sparsely phyric/ trachytic	aphyric/ trachytic
Trace element analyses (ppm)									
Ba	231	147	183	156	234	256	143	183	171
Rb	17	14	17	9	17	26	14	17	11
Sr	372	353	276	299	364	332	382	303	327
Y	42	19	30	24	40	36	20	30	29
Zr	197	111	152	118	199	209	117	157	149
Nb	16.0	6.6	11.1	8.5	17.0	17.5	8.0	10.1	9.6
Ni	7	30	7	12	3	40	40	13	16
Cu	16	108	71	95	18	154	110	153	186
Zn	111	66	78	86	114	89	69	94	87
Cr	9	70	32	29	10	76	61	30	29

Table 1. Chemical analyses of volcanic and intrusive rocks, Amboy 7.5' quadrangle—Continued

Map No.	37	38	39	40	41	42	43	44	45
Field sample No.	**00YC-P211**	**00YC-P113**	**99YC-P77**	**00YC-P194**	**00YC-P134A**	**00YC-P137A**	**99YC-P24**	**00YC-P191**	**99YC-P25**
Latitude (N) Longitude (W)	45°55.68' 122°29.76'	45°56.58' 122°27.72'	45°57.84' 122°26.40'	45°55.08' 122°29.76'	45°55.98' 122°28.02'	45°57.36' 122°23.34'	45°59.46' 122°25.98'	45°55.02' 122°23.34'	45°59.70' 122°25.62'
Map unit	Tba	Tba	Tba	Tba	Tba	Tba	Tba	Ta	Tba
Rock type	Basaltic andesite	Basaltic andesite	Basaltic andesite	Basaltic andesite	Basaltic andesite	Basaltic andesite	Andesite	Andesite	Andesite
Analyses as reported (wt percent)									
SiO_2	55.59	55.54	55.77	55.88	56.10	56.75	56.63	56.87	57.00
TiO_2	1.76	1.92	1.10	1.80	1.76	2.10	2.01	1.29	2.15
Al_2O_3	15.82	15.12	17.95	15.66	15.45	15.77	15.41	18.33	15.30
FeO*	9.72	10.37	7.61	9.85	9.75	9.24	9.38	7.46	9.13
MnO	0.18	0.19	0.15	0.18	0.19	0.19	0.20	0.16	0.19
MgO	3.81	3.54	3.88	3.44	3.75	3.34	2.94	2.63	3.18
CaO	7.71	7.55	8.51	7.61	7.61	6.91	6.32	7.60	6.69
Na_2O	3.66	3.46	3.40	3.74	3.63	4.03	4.62	4.04	4.20
K_2O	0.89	1.21	1.02	0.69	0.95	1.07	1.07	0.78	1.17
P_2O_5	0.26	0.34	0.18	0.28	0.26	0.33	0.39	0.23	0.45
Total	99.58	98.77	99.13	99.44	99.62	99.73	98.97	99.38	99.46
Analyses recalculated volatile-free and normalized to 100% with all Fe as FeO (wt percent)									
SiO_2	55.92	55.97	56.01	56.37	56.41	56.90	57.22	57.22	57.31
TiO_2	1.77	1.93	1.11	1.82	1.77	2.10	2.03	1.30	2.16
Al_2O_3	15.92	15.24	18.03	15.80	15.54	15.81	15.57	18.44	15.38
FeO*	9.78	10.45	7.64	9.94	9.80	9.27	9.48	7.51	9.18
MnO	0.18	0.19	0.15	0.18	0.19	0.19	0.20	0.16	0.19
MgO	3.83	3.57	3.90	3.47	3.77	3.35	2.97	2.65	3.20
CaO	7.76	7.61	8.55	7.68	7.65	6.93	6.39	7.65	6.73
Na_2O	3.68	3.49	3.41	3.77	3.65	4.04	4.67	4.06	4.22
K_2O	0.90	1.22	1.02	0.70	0.96	1.07	1.08	0.78	1.18
P_2O_5	0.26	0.34	0.18	0.28	0.26	0.33	0.40	0.23	0.45
Mg#	45.1	41.7	51.7	42.3	44.7	43.1	39.7	42.5	42.2
Modes (volume percent)									
Plagioclase	1.1	0.2	16.4	0.2	2.1	trace	trace	18.3	-
Clinopyroxene	0.1	trace	0.9	trace	0.5	trace	-	trace	-
Orthopyroxene	-	-	-	-	-	-	-	0.3	-
Olivine	0.1	-	1.1	-	0.5	-	-	trace	-
Fe-Ti Oxide	-	-	-	trace	-	trace	-	trace	-
Hornblende	-	-	-	-	-	-	-	-	-
Quartz	-	-	-	-	-	-	-	-	-
K-feldspar	-	-	-	-	-	-	-	-	-
Other	-	-	-	-	-	-	-	-	-
Groundmass	98.7	99.8	81.6	99.8	96.9	100.0	100.0	81.4	100.0
No. points counted	750	750	750	767	770	-	-	785	-
Texture (rock/ groundmass)	seriate/ trachytic	aphyric/ pilotaxitic	seriate/ intergranular	aphyric/ pilotaxitic	seriate/ trachytic	aphyric/ trachytic	aphyric/ intergranular	porphyritic/ pilotaxitic	aphyric/ intergranular
Trace element analyses (ppm)									
Ba	200	228	180	223	191	204	251	194	261
Rb	16	29	21	25	17	22	20	12	18
Sr	307	295	376	324	304	323	362	315	323
Y	30	35	23	38	28	34	39	31	37
Zr	154	208	138	206	157	176	210	147	224
Nb	10.4	13.5	8.7	11.7	10.2	12.5	18.7	10.0	19.2
Ni	9	12	33	5	11	0	4	2	9
Cu	317	222	80	185	172	20	96	96	125
Zn	85	97	71	94	90	86	105	81	96
Cr	23	19	53	12	26	8	9	6	17

Table 1. Chemical analyses of volcanic and intrusive rocks, Amboy 7.5' quadrangle—Continued

Map No.	55	56	57	58	59	60	61	62	63
Field sample No.	**01YC-P284**	**01YC-P347**	**99YC-P78**	**01YC-P281C**	**00YC-P197**	**01YC-P280A**	**00YC-P201**	**99YC-P17**	**00YC-P190A**
Latitude (N) Longitude (W)	45°57.78' 122°22.86'	45°53.52' 122°25.50'	45°57.78' 122°26.34'	45°58.35' 122°26.72'	45°54.54' 122°24.90'	45°58.50' 122°27.00'	45°54.52' 122°25.32'	45°53.76' 122°29.04'	45°55.14' 122°22.62'
Map unit	Ta	Ta	Ta	Ta	Ta	Tia	Ta	Td	Td
Rock type	Andesite	Andesite	Andesite	Andesite	Andesite	Andesite	Andesite	Dacite	Dacite
Analyses as reported (wt percent)									
SiO_2	58.31	58.92	59.05	60.03	60.84	60.87	61.10	65.03	65.65
TiO_2	1.34	0.90	1.40	1.49	1.36	1.55	1.31	0.72	0.75
Al_2O_3	16.09	17.38	15.92	15.17	15.72	15.14	16.04	16.12	14.74
FeO*	7.24	6.72	8.19	7.79	7.70	7.38	7.59	4.97	5.53
MnO	0.14	0.15	0.17	0.14	0.17	0.14	0.14	0.15	0.11
MgO	4.20	3.28	2.88	3.20	2.18	2.59	1.95	1.22	1.82
CaO	7.61	7.33	6.26	6.25	5.54	6.41	5.35	4.54	4.53
Na_2O	3.70	3.80	4.20	4.23	3.96	4.16	4.20	5.01	3.84
K_2O	0.66	0.83	1.04	1.08	1.62	0.71	1.50	0.84	1.86
P_2O_5	0.34	0.14	0.18	0.34	0.30	0.37	0.28	0.23	0.16
Total	99.63	99.45	99.29	99.72	99.39	99.32	99.46	98.83	98.99
Analyses recalculated volatile-free and normalized to 100% with all Fe as FeO (wt percent)									
SiO_2	58.53	59.25	59.47	60.20	61.21	61.29	61.43	65.80	66.32
TiO_2	1.34	0.90	1.41	1.49	1.37	1.56	1.32	0.73	0.76
Al_2O_3	16.15	17.48	16.03	15.21	15.82	15.24	16.13	16.31	14.89
FeO*	7.27	6.76	8.25	7.81	7.75	7.43	7.63	5.03	5.58
MnO	0.14	0.15	0.17	0.14	0.17	0.14	0.14	0.15	0.12
MgO	4.22	3.30	2.90	3.21	2.19	2.61	1.96	1.23	1.84
CaO	7.64	7.37	6.30	6.27	5.57	6.45	5.38	4.59	4.58
Na_2O	3.71	3.82	4.23	4.24	3.98	4.19	4.22	5.07	3.88
K_2O	0.66	0.83	1.05	1.08	1.63	0.71	1.51	0.85	1.88
P_2O_5	0.34	0.14	0.18	0.34	0.30	0.37	0.28	0.23	0.16
Mg#	51.1	54.9	50.6	42.4	46.3	37.3	42.4	35.0	40.8
Modes (volume percent)									
Plagioclase	23.6	31.7	3.8	4.1	0.4	1.9	7.5	9.8	5.8
Clinopyroxene	2.8	3.7	0.4	1.0	0.1	0.5	0.8	0.3	0.6
Orthopyroxene	4.8	2.5	0.4	0.2	-	0.2	trace	0.8	0.4
Olivine	-	0.4	-	0.4	-	-	-	-	-
Fe-Ti Oxide	-	0.5	0.1	0.2	trace	trace	0.1	0.2	0.2
Hornblende	-	-	-	-	-	-	-	-	-
Quartz	-	-	-	-	-	-	-	-	-
K-feldspar	-	-	-	-	-	-	-	-	-
Other	-	-	-	-	-	-	-	-	-
Groundmass	68.8	61.2	95.3	94.1	99.5	97.4	91.6	88.9	93.0
No. points counted	800	775	800	780	800	800	800	789	810
Texture (rock/ groundmass)	porphyritic/ intersertal	porphyritic/ hyalopilitic	sparsely phyric/ pilotaxitic	porphyritic/ pilotaxitic	sparsely phyric/ pilotaxitic	sparsely phyric/ intersertal	porphyritic/ pilotaxitic	seriate/ intersertal	porphyritic/ snowflake
Trace element analyses (ppm)									
Ba	254	213	208	306	313	366	316	255	365
Rb	25	18	23	39	43	35	34	36	51
Sr	357	293	337	320	226	362	233	295	198
Y	30	21	37	35	42	38	41	31	36
Zr	247	124	139	276	247	295	219	176	259
Nb	18.9	7.7	8.8	17.7	14.6	19.5	14.2	12.2	13.4
Ni	46	18	6	20	1	9	0	8	10
Cu	139	138	159	140	23	144	26	26	53
Zn	84	76	89	84	89	86	85	84	63
Cr	86	29	13	68	2	8	0	2	16

Table 1. Chemical analyses of volcanic and intrusive rocks, Amboy 7.5' quadrangle—Continued

Map No.	46	47	48	49	50	51	52	53	54
Field sample No.	**99YC-P31**	**99YC-P66A**	**99YC-P74**	**99YC-P95C**	**01YC-P349**	**99YC-P89B**	**99YC-P84**	**99YC-P39**	**00YC-P159**
Latitude (N) Longitude (W)	45°57.66' 122°28.92'	45°53.52' 122°25.14'	45°57.78' 122°26.94'	45°57.84' 122°27.36'	45°53.22' 122°25.20'	45°57.78' 122°26.10'	45°56.76' 122°26.82'	45°57.18' 122°26.34'	45°57.84' 122°23.40'
Map unit	Ta	Ta	Ta	Ta	Ta	Ta	Ta	Ta	Ta
Rock type	Andesite	Andesite	Andesite	Andesite	Andesite	Andesite	Andesite	Andesite	Andesite
Analyses as reported (wt percent)									
SiO_2	57.08	57.14	57.09	57.48	57.25	57.58	57.67	57.26	57.97
TiO_2	1.23	0.96	1.14	1.22	1.34	1.20	1.60	1.59	1.32
Al_2O_3	16.72	18.47	16.80	16.66	16.93	16.34	16.93	16.54	15.88
FeO*	7.64	7.01	7.53	7.68	8.29	7.50	8.30	8.45	7.88
MnO	0.16	0.18	0.14	0.17	0.18	0.15	0.17	0.16	0.13
MgO	4.06	3.18	4.26	3.88	3.21	4.77	2.71	2.89	3.93
CaO	7.36	8.13	7.48	7.85	7.09	7.07	6.87	6.78	7.10
Na_2O	3.55	3.56	3.60	3.74	3.97	3.65	4.18	4.08	3.49
K_2O	1.45	0.72	1.14	1.02	1.00	1.26	1.08	1.04	1.43
P_2O_5	0.23	0.13	0.19	0.22	0.22	0.23	0.32	0.32	0.34
Total	99.48	99.48	99.37	99.92	99.48	99.75	99.83	99.11	99.47
Analyses recalculated volatile-free and normalized to 100% with all Fe as FeO (wt percent)									
SiO_2	57.38	57.44	57.45	57.52	57.55	57.72	57.77	57.77	58.28
TiO_2	1.24	0.97	1.15	1.22	1.35	1.20	1.60	1.60	1.33
Al_2O_3	16.81	18.57	16.91	16.67	17.02	16.38	16.96	16.69	15.97
FeO*	7.68	7.05	7.58	7.69	8.33	7.52	8.31	8.53	7.92
MnO	0.16	0.18	0.14	0.17	0.18	0.15	0.17	0.16	0.13
MgO	4.08	3.20	4.29	3.88	3.23	4.78	2.71	2.92	3.95
CaO	7.40	8.17	7.53	7.86	7.13	7.09	6.88	6.84	7.14
Na_2O	3.57	3.58	3.62	3.74	3.99	3.66	4.19	4.12	3.51
K_2O	1.46	0.72	1.15	1.02	1.01	1.26	1.08	1.05	1.44
P_2O_5	0.23	0.13	0.19	0.22	0.22	0.23	0.32	0.32	0.34
Mg#	42.2	52.7	48.8	54.3	51.4	44.8	57.1	40.7	51.1
Modes (volume percent)									
Plagioclase	23.3	24.7	23.1	2.7	19.1	5.0	8.7	9.5	29.2
Clinopyroxene	2.5	3.2	2.9	0.2	1.1	1.1	-	-	2.7
Orthopyroxene	3.9	4.0	3.1	0.5	2.5	1.1	-	-	5.9
Olivine	-	1.4	1.0	-	-	1.8	0.1	0.1	-
Fe-Ti Oxide	0.1	-	0.2	0.2	0.4	-	0.1	0.2	0.2
Hornblende	-	-	-	-	-	-	-	-	-
Quartz	-	-	-	-	-	-	-	-	-
K-feldspar	-	-	-	-	-	-	-	-	-
Other	-	-	-	-	-	-	-	-	-
Groundmass	70.2	66.7	69.7	96.4	76.9	91.0	91.1	90.2	62.0
No. points counted	790	810	796	810	796	800	784	770	783
Texture (rock/ groundmass)	porphyritic/ hyaolpilitic	porphyritic/ intergranular	porphyritic/ intergranular	seriate/ intersertal	seriate/ intersertal	seriate/ intergranular	seriate/ intersertal	seriate/ intergranular	porphyritic/ intergranular
Trace element analyses (ppm)									
Ba	241	174	211	196	204	211	214	194	258
Rb	30	15	22	19	26	26	21	18	27
Sr	327	299	331	341	287	305	318	314	317
Y	29	20	25	25	30	29	36	34	29
Zr	198	109	159	155	147	181	193	191	248
Nb	12.4	5.8	9.2	10.5	9.5	11.3	14.3	12.4	18.5
Ni	38	22	38	27	7	75	3	9	44
Cu	160	117	87	131	113	89	99	130	63
Zn	73	70	77	80	97	80	85	87	78
Cr	59	39	74	37	14	180	5	10	77

Table 1. Chemical analyses of volcanic and intrusive rocks, Amboy 7.5' quadrangle—Continued

Map No.	64	65	66	67	68	69	70	71
Field sample No.	**99YC-P65**	**01YC-P277A**	**01YC-P282**	**01YC-P278**	**00YC-P106**	**99YC-P64**	**00YC-P124B**	**01YC-P238**
Latitude (N) Longitude (W)	45°55.86' 122°27.36'	45°58.80' 122°29.34'	45°58.08' 122°25.50'	45°58.68' 122°27.36'	45°56.64' 122°24.06'	45°56.70' 122°25.68'	45°58.26' 122°26.58'	45°54.36' 122°25.68'
Map unit	Td	Tdib	Tdib	Tdib	Tdi	Tdid	Tdib	Tdic
Rock type	Dacite	Hypersthene microdiorite	Pyroxene diorite	Microdiorite	Pyroxene diorite	Augite diorite	Pyroxene diorite	Hypersthene microdiorite
Analyses as reported (wt percent)								
SiO_2	69.59	53.21	54.20	54.61	54.95	56.42	57.53	58.19
TiO_2	0.61	1.59	1.19	1.15	1.48	1.23	1.30	0.39
Al_2O_3	15.06	16.96	17.50	17.38	16.35	17.78	15.26	20.09
FeO*	3.68	8.93	8.48	7.97	9.58	8.13	7.88	4.32
MnO	0.13	0.15	0.16	0.30	0.20	0.18	0.14	0.09
MgO	0.27	4.48	5.19	4.72	2.42	2.55	4.34	3.63
CaO	2.44	9.14	9.76	9.67	8.57	7.83	7.30	8.61
Na_2O	4.81	3.41	2.97	3.16	3.72	3.82	3.29	3.07
K_2O	2.29	1.03	0.28	0.71	0.59	0.59	1.46	0.90
P_2O_5	0.15	0.28	0.19	0.19	0.22	0.19	0.28	0.10
Total	99.03	99.18	99.92	99.86	98.08	98.72	98.78	99.39
Analyses recalculated volatile-free and normalized to 100% with all Fe as FeO (wt percent)								
SiO_2	70.28	53.65	54.24	54.69	56.02	57.15	58.24	58.55
TiO_2	0.61	1.60	1.19	1.15	1.51	1.25	1.32	0.39
Al_2O_3	15.21	17.10	17.51	17.40	16.67	18.01	15.45	20.21
FeO*	3.72	9.00	8.49	7.98	9.77	8.24	7.98	4.35
MnO	0.13	0.15	0.16	0.30	0.20	0.18	0.15	0.09
MgO	0.27	4.52	5.19	4.73	2.47	2.58	4.39	3.65
CaO	2.46	9.22	9.77	9.68	8.74	7.93	7.39	8.66
Na_2O	4.86	3.44	2.97	3.16	3.79	3.87	3.33	3.09
K_2O	2.31	1.04	0.28	0.71	0.60	0.60	1.48	0.91
P_2O_5	0.15	0.28	0.19	0.19	0.23	0.20	0.28	0.10
Mg#	13.3	51.3	56.2	55.4	34.6	39.7	53.6	63.8
Modes (volume percent)								
Plagioclase	4.3	41.9	58.7	19.5	65.1	62.2	51.5	27.1
Clinopyroxene	-	0.4	17.3	-	8.1	18.1	15.4	0.2
Orthopyroxene	0.9	5.0	5.3	-	3.6	-	3.0	2.2
Olivine	-	0.2	1.0	0.7	-	-	3.1	-
Fe-Ti Oxide	0.3	-	1.5	-	2.8	2.6	2.1	-
Hornblende	-	-	-	-	-	-	-	-
Quartz	-	-	-	-	3.2	2.2	0.4	-
K-feldspar	-	-	-	-	-	-	-	-
Other	-	-	‡interstit cl: 16.2	-	‡interstit cl: 17.2	‡qtz-fsp: 14.9	‡devit gl: 24.5	-
Groundmass	94.5	52.5	0.0	79.8	0.0	0.0	0.0	70.5
No. points counted	800	785	817	744	786	814	791	780
Texture (rock/ groundmass)	porphyritic/ snowflake	seriate/ intergranular	seriate/ intergranular	seriate/ intergranular	aphanitic/ intergranular	hypidiomorphic granular	seriate/ intergranular	seriate/ intergranular
Trace element analyses (ppm)								
Ba	394	218	134	161	169	141	262	151
Rb	56	16	2	11	9	12	28	10
Sr	175	442	362	367	289	300	287	693
Y	44	28	22	20	30	25	29	7
Zr	406	169	133	119	120	112	218	78
Nb	23.7	12.2	9.6	7.9	8.4	7.4	13.4	2.2
Ni	10	56	34	32	0	6	33	24
Cu	38	166	85	100	133	101	124	33
Zn	85	89	76	72	97	88	76	43
Cr	1	67	88	89	6	8	157	16

‡interstit cl, interstitial clay; qtz-fsp, quartz+feldspar intergrowths; devit gl, devitrified glass

Table 2. Summary of $^{40}Ar/^{39}Ar$ incremental-heating age determinations, Amboy 7.5' quadrangle

Field sample no.	Location Latitude (N)	Longitude (W)	Map unit	Rock type	Material dated	Age (±1σ error)	Source
00YC-P32	45°57.84'	122°29.04'	Qat	Tephra bed beneath till (Qat)	Plagioclase	250±36 ka	R.J. Fleck, written commun., 2003
01YC-P217A	45°53.46'	122°28.74'	Tt	Dacitic welded tuff	Plagioclase	33.0±0.1 Ma	R.J. Fleck, written commun., 2004
00YC-P206	45°54.84'	122°24.18'	Tt	Dacitic welded tuff	Plagioclase	33.4±0.4 Ma	R.J. Fleck, written commun., 2001